Alma Mater Studiorum - Università di Bologna

Medium Access Control and Routing Protocols Design for 5G

Tesi di:

Charles Jumaa Katila

Coordinatore:

Chiar.mo Prof. Ing. **Alessandro Vanelli-Coralli**

Supervisore:

Chiar.mo Prof. Ing. **Roberto Verdone**

Co-supervisore:

Dott. Ing. **Chiara Buratti**

Table of Contents

Contents

II   UAV-based beyond 5G networks   73

Abstract

In future wireless systems, such as 5G and beyond, the current dominating human-centric communication systems will be complemented by a tremendous increase in the number of smart devices, i.e., *things*, equipped with radio devices, possibly sensors, and uniquely addressable. This will result in explosion of wireless traffic volume, and consequently exponential growth in demand of radio spectrum. There are different engineering techniques for resolving the cost and scarcity of radio spectrum such as coexistence of diverse devices on the same pool of radio resources, spectrum aggregations, adoption of mmWave bands with huge spectrum, etc.

The aim of this thesis is to design and investigate advanced Medium Access Control (MAC) and routing protocols for 5G and beyond radio networks. Two main scenarios are addressed: heterogeneous scenario where scheduled and uncoordinated users coexist, and a scenario where drones are used for monitoring a given area. In the heterogeneous scenario scheduled users are synchronised with the Base Station (BS) and rely on centralised resource scheduler for assignment of time slots, while the uncoordinated users are asynchronous with each other and the BS and rely unslotted Carrier Sense Multiple Access with Collision Avoidance (CSMA/CA) for channel access. First, we address a single-hop network with advanced scheduling algorithm design and packet length adaptation schemes design. Second, we address a multi-hop network with novel routing protocol for enhancing performance of the scheduled users in terms of throughput, and coexistence of all network users.

Contents

In the drone-based scenario, new routing protocols are designed to address the problems of Wireless Mesh Networks with monitoring drones. In particular, a novel optimised Hybrid Wireless Mesh Protocol (O-HWMP) for a quick and efficient discovery of paths is designed, and a capacity achieving routing and scheduling algorithm, called backpressure, investigated. To improve on the long-end-to-end delays caused by classical backpressure, a modified backpressure algorithm is proposed and evaluated.

List of Acronyms

ACK Acknowledgement

IoT Internet of Things

BE Backoff Exponent

BER Bit Error Rate

BLER Block Error Rate

CSMA Carrier Sense Multiple Access

CSMA/CA Carrier Sensing Multiple Access with Collision Avoidance

CW Contention Window

MAC Medium Access Control

D2D Device-To-Device

PHY Physical

PLR Packet Loss Rate

HWMP Hybrid Wireless Mesh Protocol

QoS Quality of Service

RC Remote Control

PF Proportional Fair

O-HWMP Optimized Hybrid Wireless Mesh Protocol

RM-AODV Radio Metric-Ad Hoc On Demand Distance Vector

BS Base Station

LWDF Largest Weighted Delay First

UAVs Unmanned Aerial Vehicles

WSNs Wireless Sensor Networks

3GPP 3rd Generation Partnership Project

WLANs Wireless Local Area Networks

LBT Listen Before Talk

CSAT Carrier Sensing and Adaptive Transmission

CCA Clear Channel Assessment

TDM Time-Division Multiplexing

WBANs Wireless Body Area Networks

SNR Signal-to-Noise Ratio

D2D Device-to-Device

CSR Carrier-Sensing Range

HNF Hidden Neighbour Free

MLPF Multi-Link Proportional Fair

CoA Coexistence-Aware

WMN Wireless Mesh Network

EDCA Enhanced Distributed Channel Access

MCCA Mesh Coordination Function (MCF) Controlled Channel Access

STA Station

MP Mesh Point

MPP Mesh Portal Point

MAP Mesh Access Point

AP Access Point

MAR Mesh Aerial Relay

CCA Clear Channel Assessment

N-PF Neighbour-Aware Proportional Fair

CA Channel-Aware

SIR Signal-to-Interference Ratio

List of Acronyms

ETX Expected Transmission Count

ETT Expected Transmission Time

PREQ Path Request

PREP Path Reply

PERR Path Error

BP BackPressure

DSR Dynamic Source Routing

AODV Adhoc On Demand Distance Vector Routing

M-BP Modified-BackPressure

T-BP Trajectory-based BackPressure

CC Control Center

RTS Request To Send

CTS Clear To Send

DUD Discrete Uniform Distribution

List of Figures

List of Tables

Chapter 1

Introduction

This thesis is concerned with Medium Access Control (MAC) and routing protocols design for 5G and beyond radio networks. The design of these protocols is addressed in two parts. Part I addresses coexistence of heterogeneous networks, and Part II addresses drones for environmental monitoring. In both parts the scenarios considered consist of a set of fixed and or mobile nodes communicating with each other or with the Base Station (BS) in a single-hop or multi-hop. The goal of the thesis is to design efficient radio resource utilization and reliable connectivity techniques.

This chapter will provide a general introduction to the topics covered in the thesis. First, a general overview of MAC and routing protocols will be given. Second, the coexistence of heterogeneous networks, and finally, drones for environmental monitoring will be introduced.

1.1   Introduction

Future radio networks will be characterized by massive connected devices and enormous traffic volume, i.e., in the order of ZetaByte per year as predicted by Cisco [1].

The key drivers for this include but are not limited to: increased demand for broadband services and especially high quality video content [1], and the emerging Internet of Things (IoT) paradigm [2]. IoT will enable objects of everyday life, equipped with radio devices, and uniquely addressable to be connected to the Internet [3]. These objects will be connected to their respective sinks either in single or multiple hops. Despite the challenge of increased demand for radio spectrum, the resource will remain to be scarce and costly. Therefore, providing reliable connectivity to devices and addressing heterogeneous needs of these devices will be challenging. To address these problems, advanced MAC and routing protocols will be of paramount importance.

MAC and routing protocols can play significant roles in achieving efficient radio resource utilization and reliable connectivity of nodes. These protocols are designed with certain network objectives but with flexibility of trading-off one performance metric with another, for example network throughput, delay and fairness.

Finally, the coexistence of heterogeneous networks on the same spectrum and use of drones in radio networks will play significant roles in 5G and Beyond networks, hence there is need to address the engineering problem of designing MAC and routing protocols for the two areas.

1.2 Overview of Medium Access Schemes

Medium Access Control (MAC) protocol is a set of rules for regulating how a shared communication medium is accessed by a set of nodes in the network. This responsibility is designated to the MAC sub-layer of the network communication protocol stack. As shown in Fig. 1.1, MAC protocols can be classified into three main classes: contention-based, contention-free and hybrid protocols.
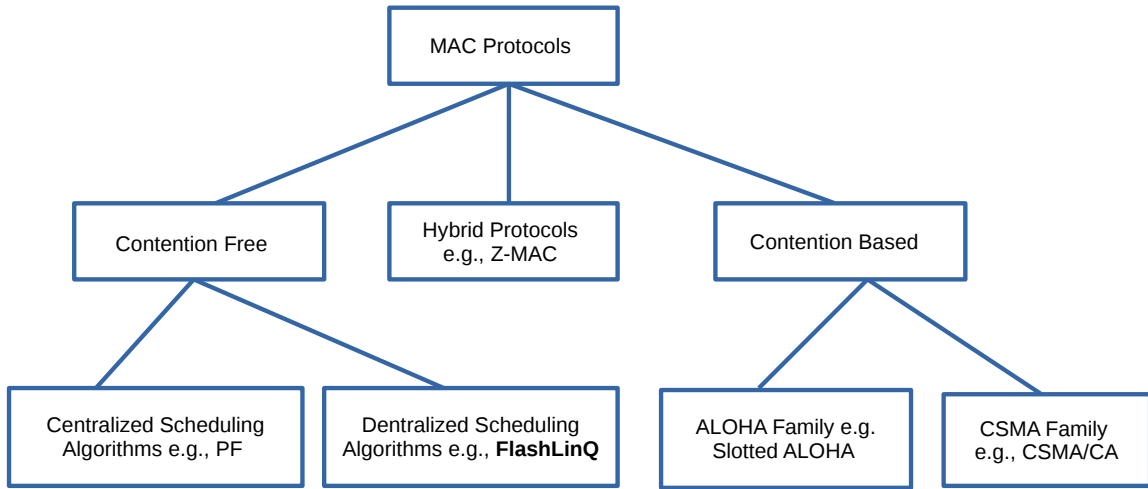
Figure 1.1: Classification of MAC protocols.

The contention-based MAC schemes suffer from packet collision problem which is resolved by random backoff algorithms. Nodes whose packets collide do not receive acknowledgements, and perform random backoff before attempting re-transmission of the lost packets. Besides collisions and re-transmissions, other sources of inefficiency are caused by: protocol overhead, idle times due to random back-off algorithms, incorrect determination of the channel state, etc.

The pure ALOHA protocol presented by Abrahamson [4], is a simple scheme where a node transmits when it has a packet ready to be sent. To improve on the throughput performance of pure ALOHA, the slotted ALOHA protocol was proposed in [5]. According to this scheme, when a node has a packet in the queue, it waits until the beginning of the next slot. The Carrier Sense Multiple Access (CSMA) family of protocols rely on both Carrier Sensing and back-off rules in order avoid collisions by distributing channel access between nodes over time. In radio networks, due to the lack of collision detection capability, the variant Carrier Sense Multiple access
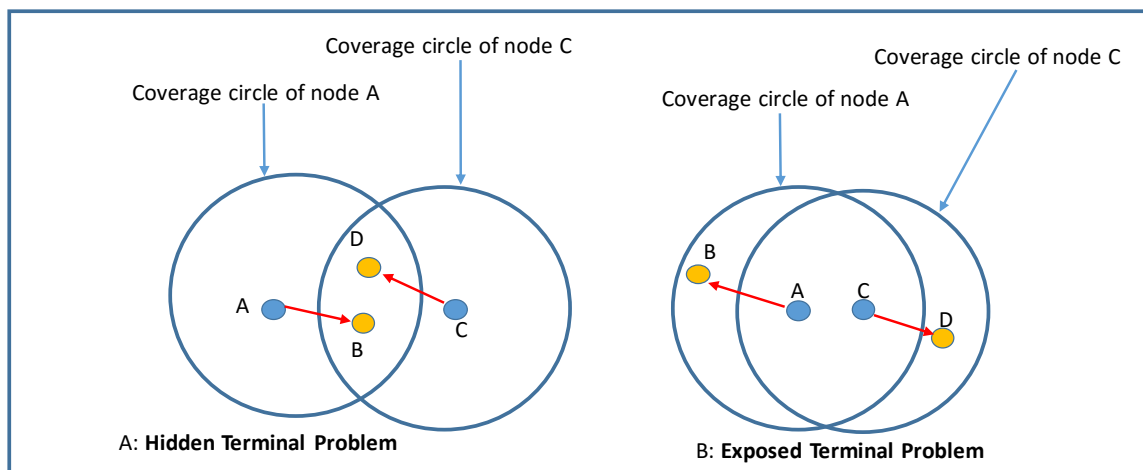
Figure 1.2: Hidden Terminal Problem.

with Collision Avoidance (CSMA/CA) is used [6]. This CSMA/CA protocol can be used in slotted and unslotted fashion and is widely applied in radio networks such as: IEEE 802.11, IEEE 802.15.4 zigbee, IEEE 802.15.6, Long Term Evolution (LTE) mobile networks, etc. However, the CSMA/CA protocol suffers from the well-know hidden and exposed terminal problems [7] which result in performance degradation.

The hidden terminal and exposed terminal problems limit the exploitation of the capacity of the radio channel. The hidden terminal effect occurs when two or more transmitters are out of coverage range of each other, while the receivers are within the coverage (interference) range of the transmitters as shown in Fig. 1.2. As a consequence, collisions occur at the receiver resulting to low throughput in the network. In the Fig. 1.2, the sender node A is out coverage of the sender node C. A want to transmit to receiver node B, and C to receiver node D. When A and B performs concurrent transmissions, collisions occurs at both receivers. This problem is resolved through the use of Request To Send (RTS) and Grant To Send (GTS) control packets as explained in [8]. On the other hand, the exposed terminal

effect occurs when a sender node willing to transmit to a receiver located outside the interference range of another transmitter is blocked from transmission hence causing unnecessary delay and channel under utilization. As shown in the Fig. 1.2, node A wants to send to node B while node C is transmitting to node D, but is blocked since node C is exposed to A.

The contention-free MAC schemes involve allocation of orthogonal or non-orthogonal resources to network users using some policies defined by the scheduling algorithm. When the network being addressed is centralised, centralised scheduling algorithms are used otherwise the schedules are developed in a distributed fashion through the exchange of control signals. In centralised systems such as the mobile radio systems, a master entity located within the Base Station (BS) is used to assign radio resources to users relying on the scheduling algorithm. In this context, the radio resources are either in time, frequency, codes or combination of more than one resource dimensions. Examples of centralised scheduling algorithms which have been widely used in radio networks include: Round-Robin (RR), Earliest Deadline First (EDF) [9], Maximum Throughput (MT),Proportional Fair (PF) [10], and Largest Weighted Delay First (LWDF) [11]. Each of these algorithms are designed to maximize or minimize some network performance metrics such as fairness, sum throughput, power consumption, latency, etc., subject to some constraints.

The hybrid MAC schemes combines the features of both the contention-free and contention-based protocols. The Zebra-MAC (Z-MAC) protocol [12] was developed for multi-hop Wireless Sensor Networks (WSNs). Similar to the Probabilistic-Time Division Multiple Access (PTDMA) protocol presented in [13], Z-MAC integrates

both CSMA and TDMA schemes to adapt to the network contention state and improve on network throughput and delay performance. In the state of low contention in the network, the protocols switch to CSMA scheme and when contention is high it switches to TDMA scheme.

1.3 Overview of Routing protocols

A routing protocol determines the shortest path between any pair of nodes in a multi-hop network, relying on a given link cost metric. There are three main classes of routing protocols: Proactive, Reactive and Hybrid protocols. Proactive routing schemes require the paths to be established and maintained before they are needed. Common proactive routing protocols include: Destination Sequenced Distance Vector (DSDV) [14], Link State Routing protocol (OLSR) [15], etc. On the other hand reactive routing protocols require routes to be established on demand e.g., Dynamic Source Routing (DSR) [16] , Ad-hoc on Demand Distance Vector (AODV) [17], etc. Hybrid schemes combine both reactive and proactive schemes.

In order to address the specific needs for a new application scenario, the routing metric component of the protocol need to be redesigned. The metric should capture the characteristics of the target network [18]. In [19] the design requirements for wireless routing metrics are presented. Some of the routing metrics which have been widely used with common routing protocols include: Hop-Count, Expected Transmission Count (ETX), and Expected Transmission Time (ETT). The Hop count is a simple channel unaware metric used with most routing protocols. However, it does not differentiate links in terms of loss rates, link rates, and interference, etc., hence it could lead to performance degradation in different target networks. The ETX metric

proposed in [20] reflect both link loss rate and path length. ETX metric is extended into ETT metric [21] to account for the link rate.

1.4   5G Heterogeneous Scenario

Heterogeneous coexistence of radio networks is a promising technique for enhancing spectrum utilization efficiency. With this approach, nodes with diverse MAC protocols coexist on the same set of radio resources. However, designing protocols for coexistence remains to be a very challenging task because of the packet collision problem which is exacerbated by lack of synchronization and coordination between the coexisting networks.

Heterogeneous coexistence of networks relies on contention-based access rules or cognitive radio principles. For fair and friendly coexistence between coexisting networks, there is need for compliance to a given set of standardized regulations. Recognizing the importance of coexistence, the IEEE 802.19 [22], IEEE 802.22 [23], and the 3rd Generation Partnership Project (3GPP) [24] groups were formed to address the issue. The 3GPP focuses on addressing coexistence between LTE and other technologies on the unlicensed bands e.g., IEEE 802.11 Wireless Local Area Networks (WLANs), IEEE 802.15.4 Wireless Sensor Networks (WSNs), and IEEE 802.15.6 Wireless Body Area Networks (WBANs), etc. The standard proposes two contention-based random access schemes as solutions to the problem: Listen Before Talk (LBT) and Carrier Sensing and Adaptive Transmission (CSAT). The LBT protocol works in a similar manner to IEEE 802.11 Carrier Sensing Multiple Access with Collision Avoidance (CSMA/CA) protocol and therefore a node captures the channel when it is deemed free according to the Clear Channel Assessment (CCA) rules.

In contrast, CSAT relies on adaptive Time-Division Multiplexing (TDM) developed based on long term carrier sensing of channel activities. Therefore, a LTE small cell is scheduled to transmit on a fraction of the cycle and then remains silent for other systems to use the channel. On the other hand, with cognitive radio approach, the secondary systems are designed to opportunistically access unoccupied/under-utilized spectrum licensed to incumbent systems (Primary Systems) [25]. The cognitive radio devices are able to change transmitter parameters according to the interactions with the environment.

In a TDM vs. CSMA coexistence, different techniques can be applied to improve on the network performance. Such techniques include: design of advanced scheduling algorithms, packet adaptation algorithms and routing protocols for multi-hop networks. The existing centralised scheduling algorithms such as the classical Proportional Fair (PF) algorithm, and Largest Weighted Delay First (LWDF) do not not capture the characteristics of coexistence networks. This makes it difficult for the scheduler to assign resources to users when chances of collisions are low i.e., the user best times for channel access. Therefore, these schedulers may not effectively take advantage of user diversity to improve on network performance unless they are redesigned.

In respect to packet adaptation techniques, scheduled users or the network controller can adapt the size trasmission packets accordingly in order to mitigate collisions, and avoid underutilization of the shared channel. In a state of low contention, nodes can transmit long packets and adaptively decrease the packet lengths with raising contention. This technique contributes to efficient utilization of the channel while respecting coexistence rules. The existing works on packet adaptation schemes

mainly address CSMA-based networks with fading channels , where packets are lost due to collisions or channel errors (low Signal-to-Noise Ratio (SNR)) [26], [27], [28] and not due to coexistence problem.

Routing protocols allows nodes to find best paths for reaching their respective sinks in a multi-hop network. Similar to the MAC protocols, the design of routing protocols is driven by the application needs in terms of performance requirements and must capture the the characteristics of the underlying network. The routing metric is the key element of the routing protocol which addresses the design requirements. In an heterogeneous scenario, the key problem to be addressed is the packet collisions caused by lack of centralised synchronization and coordination between coexisting networks. Multi-hop solution can significantly improve the performance of coexistence networks in different ways. First, nodes can be configured to transmit in short hops and at low power in order to achieve higher packet success probability and reduce level of interference in the network. Second, multi-hop communications allows for densification of the network since more nodes can be deployed on the same set of radio resources.

Part I of the thesis addresses a scenario where scheduled and Carrier Sense Multiple Access (CSMA)-based nodes coexist on the same spectrum. As depicted in the Fig. 1.3, scheduled nodes could be cellular devices (e.g., implementing Device-to-Device (D2D) communication) and the uncoordinated nodes could be IoT devices. The scheduled nodes are synchronized with the BS and rely on a centralised resource assignment scheme running at the BS, while the uncoordinated nodes are asynchronous with the BS and among themselves, and rely upon unslotted CSMA/CA protocol to access the channel. Furthermore, the scheduled nodes can communicate
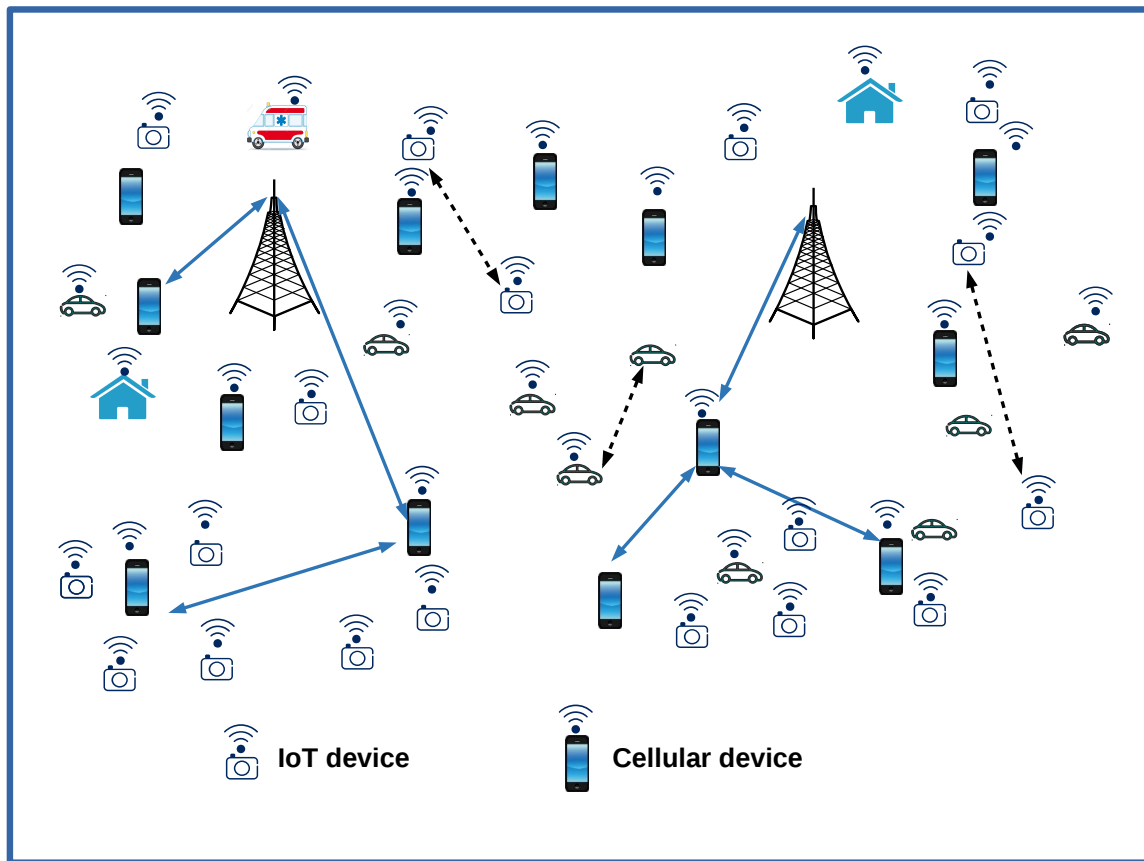
Figure 1.3: General Scenario.

with the BS either in single or multiple hops. Novel scheduling and routing algorithms are designed and evaluated.

1.5 Unmanned Aerial Vehicles Based Monitoring

The use of low altitude Unmanned Aerial Vehicles also known drones in radio networks has recently received increasing attention [29], [30], [31]. Drones are envisioned to be part of 5G and beyond networks and will enable countless services in both civilian and commercial domains [32]. Some of the potential set of services which will aided

by drones include: public safety for efficient response to disasters and emergencies, inspection of critical infrastructures and assets such as oil and gas pipelines, agriculture, environmental and wildlife conservation, logistics, flying cameras for movies and news media, improving connectivity of ground wireless devices and extending network coverage, etc.

In the IoT monitoring scenarios drones can perform several important tasks. First, a drone can act as mobile data collector where it gathers data from ground sensors and relays to the remote sink. Second, drone can serve to gather data from the environment using on-board sensors and transmit to remote sink via ground or aerial relays. In these scenarios, the drone moves from one point to another according to some predefined trajectory. Several studies have been conducted to investigate on drone placement and trajectory in different scenario in order to meet different application needs and network constraints [33], [31], [34]. Due to the ability to adjust the altitude and the mobility patterns, drones have a lot of advantages compared to ground nodes in that it can move close to other devices when needed, and can establish line-of-sight communications with relays or remote sinks. These features makes it very effective for IoT communications [29].

Currently the drone technology is faced with a lot of challenges ranging from policy and regulations to engineering design which must be addressed before its benefits can be fully realised. One of the main engineering issues is the design of resource efficient and reliable communications protocols. This challenge is attributed to the dynamic nature of network topologies caused by the drone mobility.
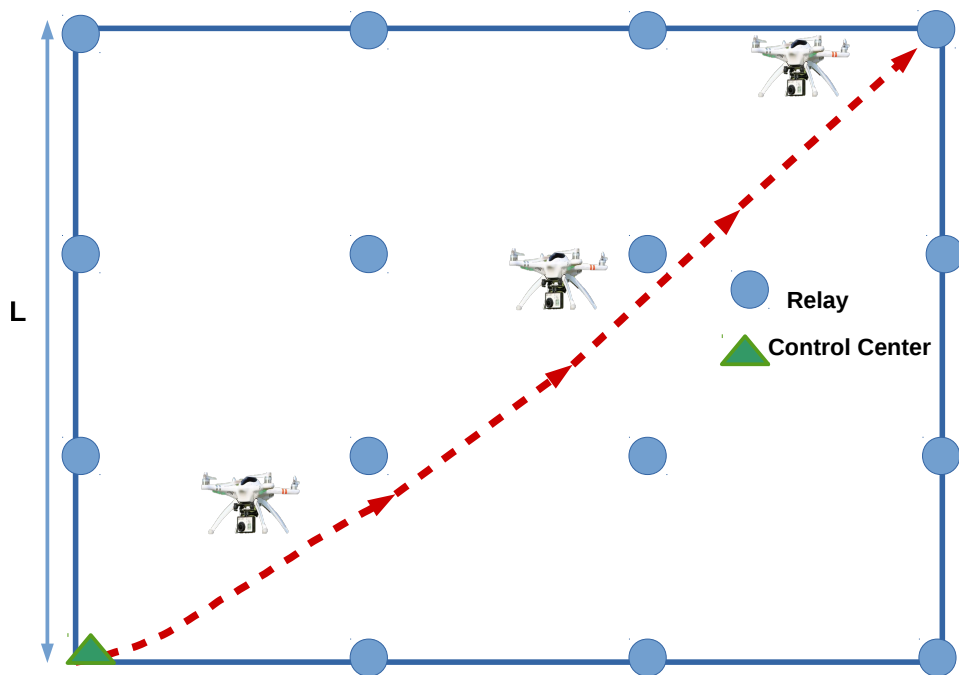
Figure 1.4: Reference Scenario.

1.6 System Model

Different from Part I, the Part II of the thesis investigates routing and scheduling protocols for multi-hop wireless networks with drones for an environmental monitoring scenario as depicted in Fig. 1.4. Unlike in Part I, where more than one type of network share common pool of radio resources, in Part II coexistence of networks on the same spectrum is not considered. As shown in Fig. 1.4, the drone is used to gather video data from the environment and transmit to a remote control center through the ground relays. A novel routing protocol denoted as Hybrid Wireless Mesh Protocol (HWMP) is proposed and evaluated. HWMP ensures quick and efficient path discovery to the Remote Control (RC). Moreover, BackPressure (BP) routing

and scheduling algorithms for multi-hop radio networks are studied considering a similar scenario, and their performance evaluated. The BP is an algorithm which relies on queue backlog differential metric for flow and link scheduling, and routing decisions. To improve the long end-to-end delay performance which characterizes the classical BP, a modified algorithm is proposed and evaluated.

In summary, this thesis investigates MAC and routing protocols design for 5G and beyond radio networks considering: 1) Coexistence of heterogeneous networks, and 2) drones for environmental monitoring. In each of the scenarios, the protocols are designed to capture the characteristics of the target network.

1.7 Structure and Contribution of the Thesis

This thesis is focused on MAC and routing protocols designs for radio networks. In particular it addresses the design of protocols for coexistence of heterogeneous networks, and drones for environmental monitoring relying on Wireless Mesh Network (WMN). It is structurally divided into two parts. Part I deals with coexistence of heterogeneous networks and consists of Chapter 2 and 3, while Part II deals with routing and scheduling in multi-hop radio networks with drones, and consists of Chapter 4 and 5. In summary, the divisions of thesis and contribution can be summarised as follows:

- Chapter 2 deals with coexistence of heterogeneous networks. In particular TDM versus CSMA coexistence on the same radio channel is addressed. This chapter is concerned with solutions for a single hop network. The problem is addressed with MAC and packet length adaptation algorithms design. In respect to MAC

protocols the work is focused on centralised scheduling algorithms for uplink communications. A lot of attention is paid to the design of the protocols to ensure that they capture the characteristics of these network scenarios. As a contribution to the existing literature, a novel centralised scheduling algorithm denoted as Neighbors-Aware Proportional Fair (N-PF), for the scheduled (TDM) nodes is proposed and evaluated. N-PF takes into account the number of potential CSMA neighbours to each of the scheduled node as apart of the aggregate scheduling metric in order to improve on packet delivery rate and goodput. Furthermore, packet length adaptation schemes solutions for mitigating collisions and enhancing the channel utilization index are investigated in the chapter.

- Chapter 3 studies an extended heterogeneous scenario presented in Chapter 2. In this scenario the scheduled nodes communicate in multi-hop in order to reach the BS. The chapter is focused on the design of routing protocols for the scheduled nodes which improve on the performance of the nodes in terms of throughput and enhance coexistence. A novel routing protocol denoted as Co-existence Aware (CA) is proposed and evaluated. The Co-existence Aware scheme takes into account the presence of CSMA-based interferers on the link as part of the link cost metric.

- Chapter 4 studies drones for video monitoring, relying on relays deployed on the ground to reach a remote control center. The nodes communicate via IEEE 802.11s WMN. A single mobile drone is used to gather video from the ground and to transmit data to the remote control center via multi-hop. This thesis is focused on the design of routing protocols for efficient and quick path discovery

which is a key requirement in video applications. As a contribution to the existing literature, a novel optimized protocol denoted as Optimized Hybrid Wireless Mesh Protocol (O-HWMP) is proposed and evaluated. The proposed scheme outperforms the standard default protocol, i.e., Radio Metric-Ad Hoc On Demand Distance Vector (RM-AODV) protocol, in terms packet success rate and end-to-end delay performance.

- Chapter 5 addresses the problem of routing and scheduling in a scenario similar to the one presented in Chapter 4. In particular, backpressure with FlashLinQ routing and scheduling schemes are investigated for this scenario. In order to improve the inherent weakness of backpressure algorithm of long end-to-end delays a modified backpressure algorithm is proposed and evaluated.

- Chapter 6 provides general conclusions.

To the best of knowledge of the author, no prior research work in literature has addressed the above mentioned points.

Part I

Scheduling and routing in heterogeneous Radio Networks

This part of thesis is focused on heterogeneous coexistence problem where users with diverse MAC Protocols coexist on the same spectrum. The concern of the work is the design of communication protocols for enhance the performance of the coexisting networks. The problem is addressed with three different techniques namely, MAC protocols design, packet-length adaptations schemes, and routing protocols design. These solutions attempts to capture the characteristics of the scenario in order to minimise interference and improve on radio resource utilization. Chapter 2 addresses single-hop solutions, while Chapter 3 addresses multi-hop solutions.

Chapter 2

Single-Hop Network Solutions

This chapter discusses communication protocols design solutions for a single-hop heterogeneous networks. In particular, the work is focused on the design of MAC and Packet-length adaptations algorithms. MAC solutions have performance limit in resolving the coexistence challenge, and this motivates the need for combination of more than one technique.

2.1 Introduction

The paradigm of spectrum coexistence allows users with diverse MAC protocols to coexist on the same set of radio resources [24] based on some set of rules. This has been prompted by the scarcity of radio spectrum, and the predicted exponential growth of the devices to be connected to the internet via radio links generating huge traffic volume in future networks. Currently, coexistence is addressed with contention-based approaches [35] or cognitive radio approaches [36]. For fair and friendly coexistence between the involved networks and to protect incumbent systems on the spectrum, the

communication protocols must be designed in compliance with existing standardized rules. The 3GPP [24], IEEE 802.19 [22], 802.22 [23], 802.11af [37] groups have focused on addressing the issue.

The main challenge in the design of coexistence protocols is the presence of uncontrolled interference on the communication links. This occur due to lack of synchronization and coordination between the coexisting networks making it impossible to completely eliminate collisions and packet losses. In contention-based aided coexistence, the problem of packet collisions is worsened by the hidden terminal problem [7]. However, for a scheduled network, it is possible to estimate which user in the network is likely to have higher packet capture success probability if assigned a transmission resource, and hence the need for designing appropriate scheduling algorithms. The details of scheduling algorithms are never specified by radio standards but left as vendor specific problem [38]. Moreover, collisions and channel underutilization could be mitigated by optimal packet length adaptation algorithms.

Based on the above motivation, this chapter addresses a scenario, where two types of users coexist on the same set of radio resources: scheduled users (hereafter denoted as *scheduled nodes*) synchronized and coordinated by a BS, and uncoordinated users (hereafter denoted as *uncoordinated nodes*), asynchronous with the BS and among them. As shown in Fig. 1.3, scheduled nodes could be user equipment (i.e., cellular users), while uncoordinated nodes could be things of the Internet of Things (IoT), i.e., cars, machines, buildings, etc. [2]. The scheduled nodes rely on a centralised resource allocation algorithm located at the BS for time slot assignment, while the uncoordinated nodes rely on unslotted CSMA/CA protocol for channel assignment. The aim to minimize the interference caused by uncoordinated nodes on the scheduled

nodes. Collisions between scheduled and uncoordinated nodes may arise under three circumstances:

- A scheduled node starts a transmission simultaneously with one or more uncoordinated nodes;

- Uncoordinated transmission(s) starts while scheduled transmission is still ongoing due to the hidden terminal problem;

- A scheduled transmissions starts while uncoordinated transmission(s) are still ongoing.

In order to avoid starvation of the uncoordinated nodes, the scheduled nodes are enforced to capture the channel at the beginning of slots for which they are assigned, while uncoordinated nodes are allowed to capture the channel at any time when it is deemed free according to the CSMA/CA procedure. Moreover, each scheduled node occupy the channel only for a fraction of the slot assigned to it and then remains silent for the remaining fraction to allow uncoordinated nodes to occupy the channel. The time frame is designed as depicted in the Fig. 2.5.

In summary, the focus of the chapter is to design a centralised scheduling algorithm and a packet length adaptation algorithm for improving the performance of the scheduled nodes while enhancing coexistence with other nodes. The work concentrates on the performance of the scheduled nodes when immersed in a set of uncoordinated nodes sharing the same spectrum. Therefore, it is important to underline that all algorithms proposed are for the scheduled nodes, and designing new algorithms for the uncoordinated nodes is out of scope of this work.
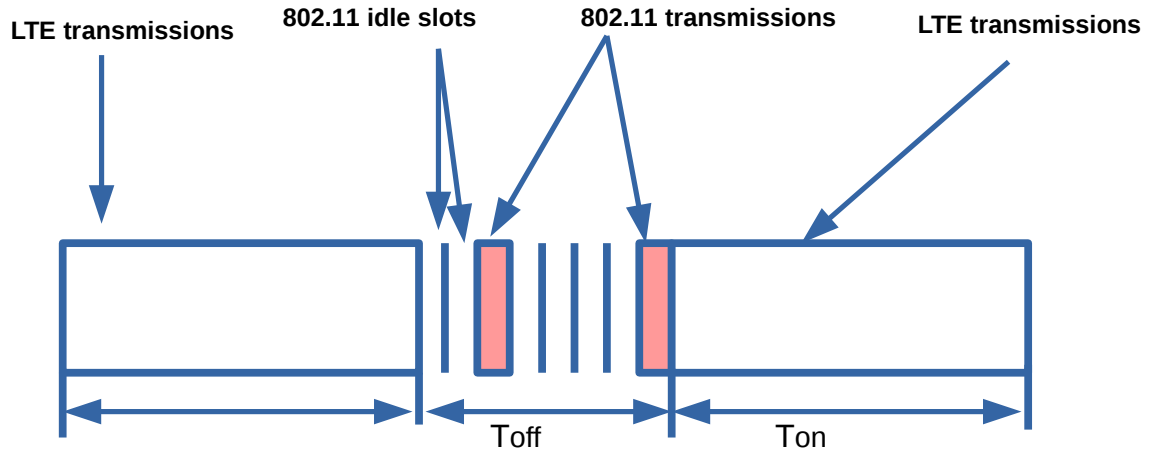
Figure 2.1: Schematic showing LTE-CSAT/802.11 transmission timing.
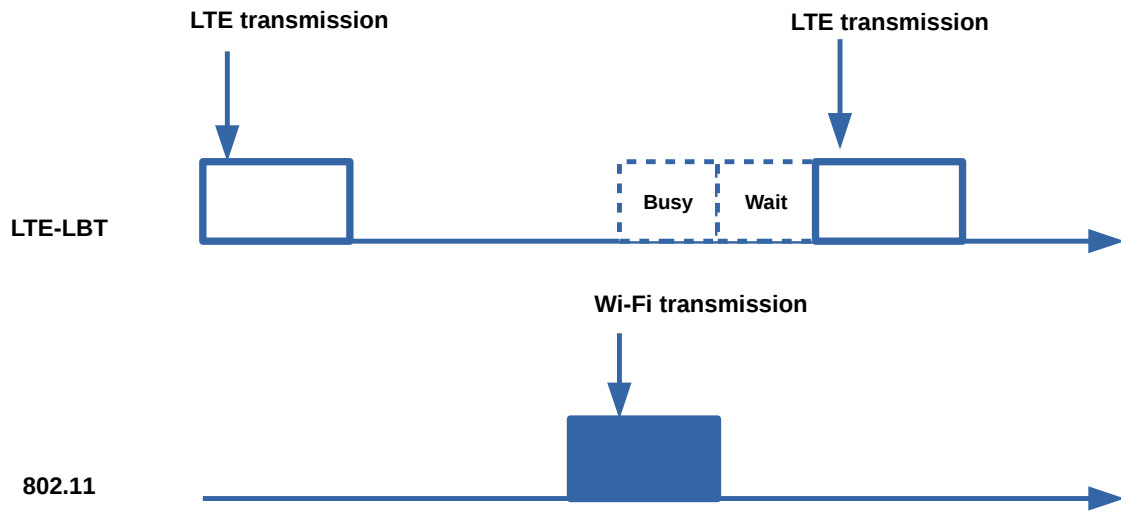
Figure 2.2: Schematic showing LTE-LBT/802.11 transmission timing.
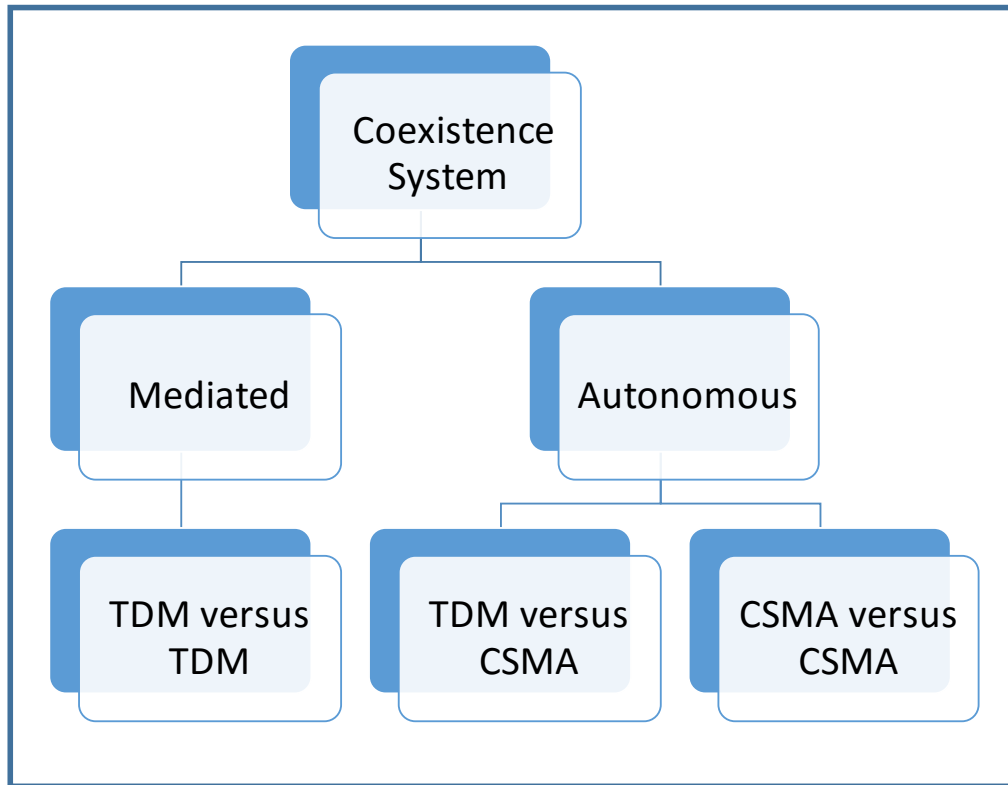
Figure 2.3: Taxonomy of coexistence schemes [39].

2.2   Related Literature

This section provides a brief review of literature on MAC protocols in general, heterogeneous coexistence of MAC schemes, and packet length adaptation schemes.

2.2.1   Coexistence of Heterogeneous MAC schemes

In the past, a lot of research studies have been done on coexistence of heterogeneous access schemes. However, this topic continues to attract increasing interests from

the scientific and industrial communities because of its promising potential in IoT and beyond-5G networks. Authors in [39] classify the coexistence schemes into two main classes: mediated and autonomous coexistence. In mediated class, there is a network entity which serves as mediator between the coexisting networks to facilitate fair coexistence and mitigate collisions. The mediator also helps to ensure tight synchronization and coordination of the involved networks. This type of coexistence is applicable when two or more Time-Division Multiplexing (TDM) systems share common channel. On the other hand, autonomous coexistence does not need any coordination of the involved networks. In this class we have TDM vs. CSMA and CSMA vs. CSMA networks. The classification is summarised by the Fig. 2.3. This chapter focuses on the TDM versus CSMA coexistence.

The 3rd Generation Partnership Project (3GPP) proposes two main mechanisms for fair co-existence of LTE, WiFi and other technologies in the unlicensed spectrum: Listen Before Talk (LBT) and Carrier Sensing and Adaptive Transmission (CSAT) [35]. The CSAT scheme develops TDM frame with active and silent periods based on long term carrier sensing. LTE BS transmits in active portions of time and vacates the channel for other technologies in the silent portions of the frame. Therefore, CSAT allows TDM-based nodes (LTE network) coexist with random access based nodes (WiFi or other technologies) on the same channel. Figs. 2.1 and 2.2 depicts 3GPP standardized protocols, the LBT and the CSAT respectively. Different from these works, this research address the design of uplink centralised scheduling algorithms for the scheduled nodes in a TDM vs. CSMA coexistence scenario.

There are several works in literature addressing spectrum sharing and coexistence

using the cognitive radio technique [36]. This approach allows the coexistence of primary (licensed) users and the secondary (cognitive) users on the same channel. The secondary users opportunistically access under-utilized spectrum licensed to incumbent systems [40]. Authors in [41] study the problem of heterogeneous coexistence between TDM and CSMA networks in TV White-Space (TVWS) spectrum, and address hidden terminal problem with a beacon transmission mechanism. Centralized scheduling in cognitive radio networks is studied in [42, 43]. These works are different from the studies carried out in this thesis because, according to the scenario under study neither the scheduled nor the uncoordinated nodes rely on cognitive radio principles to enhance coexistence.

The IEEE 802.15.4 MAC provides an option for a TDMA mode which operates without carrier sensing. Authors in [44] study the problem of coexistence between ZigBee and TDMA MAC and WiFi. The work proposes a new paradigm which relies on busy tone signals to enhance the mutual observability between ZigBee and WiFi in order to improve on coexistence. The Time-Slotted Channel Hopping (TSCH) protocol proposed in IEEE802.15.4e standard is expected to coexist with random access schemes used by other technologies in the unlicensed bands [45]. TSCH-based devices can mitigate interference and fading through channel hopping technique. Traffic aware scheduling algorithm for reliable low-power multi-hop IEEE 802.15.4e networks is studied in [46]. The authors propose a new scheme based on graph theory method of matching and coloring. The Probabilistic TDMA (PTDMA) [47] and Z-MAC [12] protocols are hybrid access schemes which combine features of both TDMA and CSMA. They are designed with the flexibility to switch between CSMA and TDMA based on the state of contention in the network. According to these schemes, each node in the

network is assigned a time slot to transmit but it could capture the channel on any other slot after performing CSMA procedure. Similarly, authors in [48] propose an hybrid MAC protocol for heterogeneous Machine to Machine (M2M) networks which combine features of contention-based and TDMA schemes. A spectrum-aware cluster-based energy-efficient routing hybrid scheme is discussed in [49]. In this scheme, the TDMA and CSMA operate on different channels.

In summary, with respect to the MAC protocols, the scope of this chapter was to design and evaluate a centralised resource scheduling algorithm for the scheduled nodes in a scenario where scheduled nodes and uncoordinated nodes coexist on the same set of radio resources. A new algorithm, called Neighbours-Aware proportional fair, was proposed and its performance evaluated. The Neighbours-Aware proportional fair algorithm takes into account both the channel quality information and the number of the uncoordinated nodes neighbouring each of the scheduled nodes in the aggregate scheduling metric to improve on the performance of the network in terms of packet delivery rate and Jain index [50].

2.2.2 Packet Length Adaptation

The literature on packet length adaptation schemes is extensive, and especially on 802.11 WLANs [28,51]. However, very few works exploit packet size adaptation in an heterogeneous coexistence of scheduled and uncoordinated nodes on the same channel to enhance the performance of one or both of the user groups involved. Furthermore, most of the existing works account only for channel errors which occur due to the time varying SNR on links and neglect the effects of hidden terminals. In [26,52], Authors propose a loss-based packet length adaptation algorithm for IEEE.802.11 WLANs

with hidden terminals operating in a time-varying wireless channel. The Authors have shown that, accounting for the effect of hidden terminals in the packet loss models can improve the throughput significantly. In [53], Authors consider IEEE.802.11b WLAN under interference from IEEE 802.15.4 network. The authors demonstrate that, packet length optimization can result in improved throughput in presence of interference. Dynamic packet size optimization and channel selection for cognitive radio sensor networks is studied in [54]. Finally, [27] studies frame aggregation schemes in 802.11n WLAN with channel errors, and proposes optimal frame size adaptation algorithm.

In this chapter, a new packet length adaptation scheme, denoted as Channel-Aware (CA), for the scheduled nodes is proposed and evaluated. The scheme takes advantage of the capture effect phenomenon [55] to improve on goodput of the scheduled nodes. Nodes are assigned packet sizes depending on the position with respect to the BS. The algorithm is clearly explained in Sec. 2.7. However, this algorithm results in reduction of time meant for exclusive transmission by uncoordinated nodes especially when scheduled nodes close to the BS are transmitting.

2.3   Contribution and Structure of the Chapter

This chapter makes contributions to the current problem of heterogeneous coexistence. In summary, the contribution of the chapter include:

- A new problem where scheduled nodes coexist on the same pool of radio resources with uncoordinated nodes;

- A novel centralized resource scheduling algorithm, called Neighbors-Aware Proportional Fair (N-PF), which takes into account the relative channel quality metric, and the relative neighborhood metric accounting for the presence of uncoordinated nodes in the cell is proposed and evaluated against a given benchmark based on PF scheduler;

- A novel packet length adaptation algorithm, called Channel-Aware (CA) algorithm, is proposed and evaluated against a given benchmark scheme, denoted as Discrete Uniform Distribution (DUD) algorithm.

The impact of CSMA parameters (e.g., CCA threshold, and Backoff Exponent (BE)) on the protocols, is also evaluated.

The rest of the chapter is organized as follows: Section 2.4 discusses Problem Statement, Section 2.5 describes the system model, Section 2.6 describes the benchmark and the proposed scheduling algorithms, Section 2.7 describes the packet length adaptation schemes, Section 2.8 describes the implementation, Section 2.9 reports numerical results and, finally, Section 2.10 provides conclusions of the chapter.

2.4   Problem Statement

Due to the lack of synchronization and coordination between the scheduled and uncoordinated nodes, collisions can not be fully avoided but could be minimized. Two main types of collisions could arise: full overlap and partial overlap collisions. The full overlap collisions arise when scheduled and uncoordinated nodes start transmitting simultaneously, while partial overlap collisions occur when a scheduled or uncoordinated node starts transmissions first and then interrupted by the other. The

performance of a scheduled node strongly depends on the position of the node with respect to the BS, and the number of uncoordinated nodes neighbouring the node, i.e., the uncoordinated nodes whose the scheduled node is within the Carrier-Sensing Range (CSR). Scheduled nodes experiencing bad channel conditions due fading and the distance with respect to the BS, may perform very poorly in this kind of networks depending on the number of uncoordinated nodes accessing the shared channel. The problem is exacerbated by the presence of hidden terminals in the network. Poor resource allocation algorithm can result into poor overall network performance. The problem for the design of the scheduling algorithm can be stated as follows:

Problem. *Given a set of scheduled nodes $\mathcal{N}$, indexed as $i = 1, 2, ..., N$, sharing the same channel with a set of uncoordinated nodes $\mathcal{M}$, and a set of T time slots $\mathcal{T}$, where $T < N$. How should the scheduler assign slots to scheduled users at each scheduling instance so as to maximize network throughput while ensuring long term fairness.*

It is important to underline that: 1) in the problem statement above none of users rely on cognitive radio principles for medium access, 2) this section describes only the scheduling algorithm problem

2.5 System Model

2.5.1 Reference Scenario and Radio Resources

An uplink scenario in a single square cell of side L m, consisting of N scheduled nodes, M uncoordinated nodes, a single BS placed in the center of the cell, is considered. All nodes are randomly and uniformly distributed within the cell as shown in Fig.
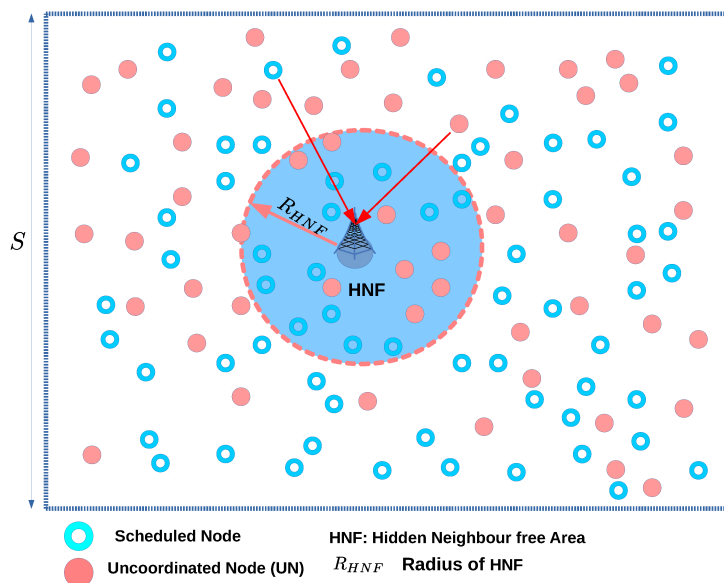
Figure 2.4: System model.

2.4. Radio resources are in the form of Time Division Multiple Access (TDMA) slots (hereafter referred as slots). In particular, time is divided into frames, composed of T slots, each subdivided into a equally sized sub-slots (see Fig. 2.5). When a scheduled node is assigned a slot to transmit, its transmissions begin at the boundary of that slot and occupies the channel only for a fraction of the slot, g sub-slots, leaving the remaining fraction for possible uncoordinated nodes transmissions. Therefore with this paradigm, a scheduled node can only access the channel in the first part of the slot, while an uncoordinated node is not restricted and accesses the channel depending on the CSMA/CA protocol.

2.5.2 Traffic Model

For the purposes of evaluation of the protocols we choose the Poisson arrival process traffic model. According to the model, all nodes generate packets with arrival rate λ
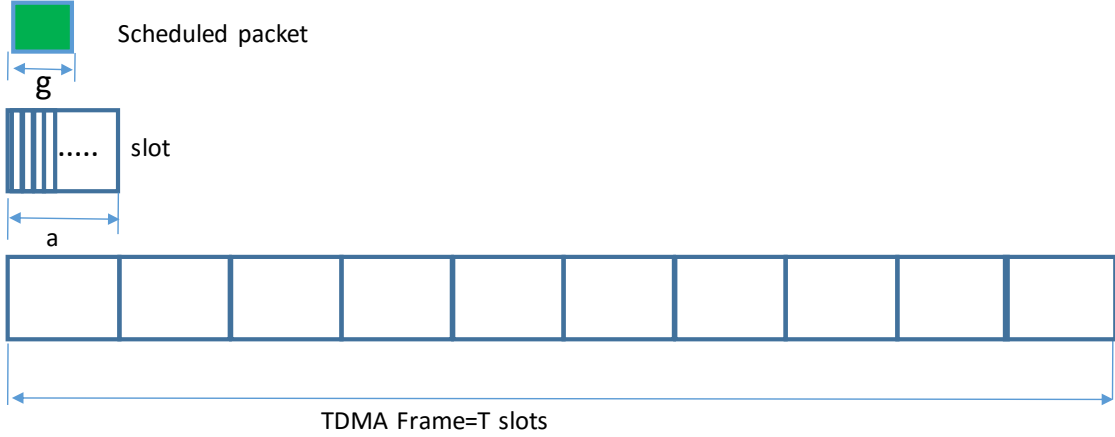
Figure 2.5: Time frame structure and packet transmission times.

[bytes/frame]. Regarding to the packet length, uncoordinated nodes transmit equal length packets of L bytes, while scheduled nodes transmit fixed-length packets when no packet length adaptation algorithm is used and variable packet length when packet length adaptation algorithms are used. The packet length adaptations algorithms are described in Section 2.7.

2.5.3 Channel and Packet Capture Models

Let P_T and P_R denote the transmit and received powers respectively, then P_R is given by:

$$P_R[dBm] = P_T[dBm] - P_L[dB] \tag{2.5.1}$$

where P_L is the path-loss between the transmitter and the receiver. If we let i be a network node connected to the base station, then i is affected by path-loss, P_{L_i}, according to the following model

$$P_{L_i}(d)[dB] = k_0[dB] + k_1 \log_{10} d(i, BS) - \gamma_i[dB] \tag{2.5.2}$$

where k_0 is the path-loss at 1 meter given by: $20 \log_{10} \frac{4\pi}{\Lambda}$, where Λ is the wavelength and $k_1 = 10 \cdot \eta$, being η the propagation path-loss exponent dependent on the environment, and $d(i, BS)$ is the distance between user i and the base station. In linear scale, γ_i is an exponentially distributed component with unit mean, accounting for Rayleigh fading effect on the link.

It is assumed that a packet is correctly received if the conditions given below are satisfied:

1) No Physical Layer (PHY) issues are present. For a given packet of interest, we first compute the packet error probability, p_e, due to PHY layer, assuming that no forward error correction is applied, is given by

$$p_e = 1 - (1 - BER)^l \tag{2.5.3}$$

where l is the number of bits transmitted (i.e., $l = L * 8$), BER is the bit error rate, which depends on the modulation scheme used. In the model a Quadrature Phase Shift Keying (QPSK) modulation is adopted, and hence,

$$BER = \frac{1}{2} erfc(\sqrt{SNR}) \tag{2.5.4}$$

where $erfc$ is the complementary error function, and SNR is the signal-to-noise ratio in linear units, given by

$$SNR = P_R[W]/P_n[W] \tag{2.5.5}$$

where P_n is the noise power. The PHY layer issues happens with probability p_e.

2) If no PHY layer issues are present, then we check if $SIR \geq \alpha$ for the entire duration of packet transmission. Where α is the protection ratio (also denoted as capture threshold) and SIR is the signal-to-interference ratio metric.

Finally, we assume that an uncoordinated node i is a neighbor of a scheduled node j if i can 'hear' transmissions of j, that is: $P_R \geq CCA_{thr}$, where CCA_{thr} is the Clear Channel Assessment (CCA) threshold. Let $\mathcal{N}_{j_n} = \{1, 2, ..., n_j\}$ denote the subset of all uncoordinated nodes neighboring j. The properties of $\mathcal{N}_{j_n}$, i.e., cardinality of the subset and its elements change according to the coherence time of the channel because of Rayleigh fading effect on links. Therefore $\mathcal{N}_{j_n}$ has a minimum and a maximum cardinality of 0 and M, respectively.

2.5.4 The CSMA/CA protocol

It is out of scope of this work to propose a novel CSMA/CA protocol; therefore, the protocol whose flowchart is reported in Fig 2.6 is considered. Before transmission, the contending nodes sense the channel to determine whether is busy or idle: the channel is determined to be busy if the level of sensed power in the channel is above a certain CCA threshold, CCA_{thr}. At the beginning of backoff process for a given node, the node selects randomly and uniformly a backoff delay time from the contention window as

$$\mathcal{U} \sim [0, 2^{BE} - 1] \tag{2.5.6}$$

where $\mathcal{U}$ denotes uniform distribution, and BE is the backoff exponent set to a fixed value (see Tab. 2.1). As in the case of many CSMA/CA protocols a maximum number of backoff stages, NB_{max}, is imposed, after which the channel access attempt is considered to have failed. Finally, retransmissions of lost packets are not considered.
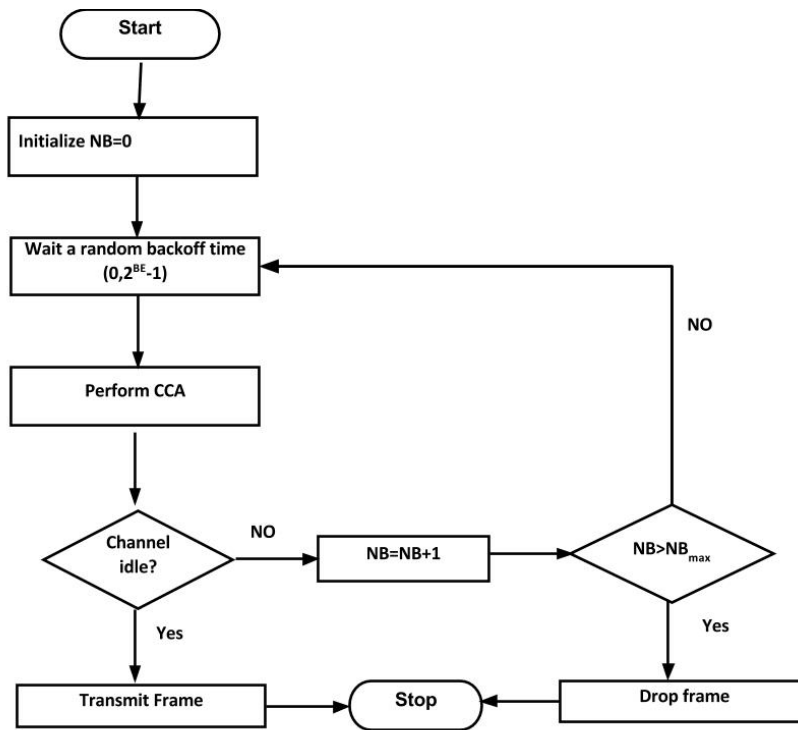
Figure 2.6: The CSMA/CA protocol.

2.6 Scheduling Algorithms

In this Section the benchmark protocol, that is Proportional Fair, and the proposed solution are described.

2.6.1 Benchmark Scheduling Algorithm: Proportional Fair

Wireless networks are characterized by time varying channel conditions, which are independent for different users. The proportional fair algorithm is designed to take advantage of multi-user diversity, while maintaining comparable long term throughput

for all users. Let $R_j(t)$ denote the instantaneous data rate that user j can achieve at time instant t, and $\underline{R}_j(t)$ be the average throughput for user j up to time slot t. The proportional fair scheduler selects the user, denoted as j^*, with the best relative channel quality according to the metric $R_j(t)/\underline{R}_j(t)$ for transmission. The average throughput $\underline{R}_j(t)$ for all the users is updated as:

$$\underline{R}_j(t+1) = \begin{cases} (1-\beta)\underline{R}_j(t) + \beta R_j(t), & j = j^* \\ (1-\beta)\underline{R}_j(t), & j \neq j^* \end{cases} \qquad (2.6.1)$$

where $0 \leq \beta \leq 1$ and $1/\beta$ is the averaging time window [56]. By changing β the scheduler can trade off between the throughput of the system and temporal fairness among the users. In this work, R_j is computed according to the normalized Shannon capacity formula as $\log_2(1 + SNR)$.

2.6.2 Proposed Scheduling Algorithm: Neighbour-Aware Proportional Fair

The PF algorithm is modified encapsulating into the scheduling metric the number of uncoordinated nodes neighboring each scheduled node. At time instant t, our proposed algorithm N-PF, selects the user, denoted as j^*, with the largest aggregate scheduling metric given as:

$$\frac{R_j(t)}{\underline{R}_j(t)} * \left(\frac{1}{\Omega_j(t)}\right)^\rho \qquad (2.6.2)$$

where $\rho \geq 0$ is an optimization constant used by the scheduler to emphasize or de-emphasize relative neighborhood metric Ω_j during scheduling. For $\rho = 0$, the algorithm turns to be the PF algorithm. For higher values of ρ, the term $1/\Omega_j(t)$ becomes predominant. For a given scheduled node j and with perfect knowledge of

the number of its uncoordinated neighbors $(n_j(t))$ at time instant t, $\Omega_j(t)$ is given by:

$$\Omega_j(t) = \begin{cases} 1 - \left(\frac{n_j(t)}{M}\right), & M > 0 \ \& \ n_j(t) \neq M \\ b, & M > 0 \ \& \ n_j(t) = M \\ 1, & M = 0 \end{cases} \tag{2.6.3}$$

where M is the total number of uncoordinated nodes deployed in the cell and b is an arbitrarily small positive constant.

2.7 Packet Length Adaptation Schemes

The benchmark packet length distribution considered in this, that is, Discrete Uniform Distribution (DUD), is described and then the proposed solution is reported.

2.7.1 Benchmark Scheme: Discrete Uniform Distribution

The benchmark packet length selection algorithm is based on a discrete uniform distribution of packet lengths. In this scheme, a scheduled node selects a packet length, L, to transmit according to

$$L \sim \mathcal{U}\big[L_{min}, L_{max}\big] \tag{2.7.1}$$

where L_{min} and L_{max} are the minimum and maximum possible packet sizes in bytes supported. The difference between two consecutive packet sizes in the ordered set is a fixed constant ΔL which is set to L_{min} in the rest of this chapter.

2.7.2   Proposed Scheme: Channel-Aware Packet Length Adaptation

In collision prone CSMA-based wireless networks with hidden terminals, packet length adaptation schemes can play an important role in mitigating the effects of collisions. Losses of long packets due to collisions can result in significant waste of network radio spectrum and energy [57]. The probability of packet collisions and hence losses due to the presence of hidden terminals increases with packets size. This can be attributed to the fact that, when the packet length increases the set of hidden terminals for a given node has to remain silent for longer time in order to avoid collisions. Similarly, as the number of hidden terminals increases, the chance of collision and losses increases due to the increased average number of transmissions from the set of hidden terminals. In such a condition, small packets transmission are favourable, but if not carefully optimized based on the wireless channel conditions, it can result in low network throughput and channel under utilization.

The CA algorithm is designed for the scheduled nodes only. It aims at achieving high throughput by assigning long packet transmission opportunities to those scheduled nodes within the Hidden Neighbour Free (HNF) area (see Fig. 2.4). The HNF area is a circle, centered at the BS, where all scheduled nodes within that region do not suffer from the hidden terminal problem resulting from the uncoordinated nodes in the region. This is because all uncoordinated nodes in the HNF can sense any scheduled transmission emanating from within the region. The radius of of HNF, R_{HNF}, is given by:

$$R_{HNF} = \frac{\tilde{R}_s}{2} \tag{2.7.2}$$

where $\tilde{R}_s$ is the approximated carrier sensing range in meters, computed by adding a fading margin, γ_f:

$$\tilde{R}_s = 10^{\frac{P_T - (CCA_{thr} + \gamma_f) - k_0}{k_1}} \; [m] \tag{2.7.3}$$

where k_0 and k_1 assume the same meaning as in eq. (2.5.2).

A scheduled node j belongs to the HNF area if the SNR estimated at the base station (SNR_j) based channel state information is greater than a given threshold (ξ), i.e.,

$$SNR_j \geq \xi \tag{2.7.4}$$

where ξ is the SNR threshold in dB given by:

$$\xi = P_T - (k_0 + k_1 \log_{10} R_{HNF}) - P_n \tag{2.7.5}$$

and P_n is the noise power in dBm. Therefore, if the link quality of a given node j is high such that $SNR_j \geq \xi$, the node is considered to belong to the HNF area regardless of its physical location in the cell. Within HNF area almost all uncoordinated nodes in the region can sense any ongoing scheduled transmission within the region and refrain from accessing the channel. Moreover, the packet capture success probability of the scheduled nodes in the region is very high even in the presence of concurrent uncoordinated transmission(s) from outside the HNF area. The CA algorithm runs within the BS to determine appropriate packet lengths for the scheduled nodes: nodes in the HNF area are assigned maximum allowable packet length, L_{max}, while those outside the HNF area are assigned packet lengths randomly and uniformly distributed between L_{min} and L_{max}, according to the DUD algorithm.

2.8   Simulation Environment

2.8.1   Simulator and Parameters

A C++ simulator implementing the algorithms and the system model described above has been used. The scenario implemented consist of a square cell of length 1000 m, a single BS placed at the center of the cell, and variable number of scheduled and uncoordinated nodes which are randomly and uniformly distributed in the cell. It is assumed that all nodes have omnidirectional antennas. There is a single frequency channel which is partitioned into time frames with each frame consisting of 10 equal slots. Each slot is further subdivided into 200 equal sub-slots of $80\mu s$ duration. Within each sub-slot only 10 bytes of traffic can be transmitted. The path-loss is computed as given by the path-loss model in equation (2.5.2) with k_0 and k_1 set to 40.7 dB and 30, respectively. For both types of nodes the traffic arrival rate is set to 500 bytes per frame. Uncoordinated nodes always transmit packets of fixed length set to 50 sub-slots (i.e., 500 bytes), while scheduled nodes transmit either fixed-length or variable-length packets depending on whether the packet adaptation algorithm is used or not. The resource scheduling algorithm runs at the beginning of each new frame. Each scheduled node requesting for resources is assigned a maximum of one slot per frame. The parameters of the CSMA/CA protocol and other default parameters used in this simulation are summarized in Table 2.1. A single simulation consists of 1000 frames. Results are averaged over 10 different simulation scenarios, characterized by different nodes' positions in the area.

Table 2.1: Default Simulation Parameters

Parameter	Value
β	0.1
M	50 nodes
N	100 nodes
Packet length	50 sub-slots
L_{max}	200 sub-slots
L_{min}	10 sub-slots
S	1000 m
Fade margin (γ_f)	5 dB
Bit Rate	1 Mbps
SIR threshold (α)	3 dB
BS height	20 m
NB_{max}	10
CCA threshold (CCA_{thr})	$-85dBm$
CCA duration	8 sub-slots
Contention Window (CW)	31 sub-slots
1 sub-slot	$80\mu s$
BE	5
b	$0.1/M$
Channel coherence time	10 slots

2.8.2 Performance metrics

1. **Jain Index (JI)** [58], given as

$$Jain\ Index = \left(\sum_{j=1}^{N} x_j\right)^2 \Big/ \left(N \sum_{j=1}^{N} x_j^2\right) \qquad (2.8.1)$$

   where x_j is the average number of radio resource units i.e., slots, allocated to user j within an interval of 1000 frames.

2. **Packet Delivery Rate (PDR)** is given by:

$$PDR = \frac{n^o\ of\ successful\ packets}{n^o\ of\ transmitted\ packets} * 100 \qquad (2.8.2)$$

3. **Blocking Rate (BR)**: if we let U_A be the number of unsuccessful channel access attempts and T_A be the total number of channel access attempts, where a channel access attempt is unsuccessful if a node fails to capture the channel after reaching maximum allowable retries, then BR is then given by:

$$BR = \frac{U_A}{T_A} * 100 \qquad (2.8.3)$$

   BR estimates the level of inhibition in the access to the channel suffered by CSMA-based nodes.

4. **Network Goodput (NG)** is given by:

$$NG = \frac{correctly\ received\ bits\ in\ N\ frames}{time\ duration\ for\ N\ frames}$$

   where at the numerator we have the sum of the number of bits correctly received at the BS when transmitted by the N scheduled nodes (NG for scheduled nodes) or by the M uncoordinated nodes (NG for uncoordinated nodes).

5. **Channel Utilization Index (CUI)** is given by:

$$CUI = \frac{Aggregate\ Goodput}{Bit\ Rate}$$

where aggregate goodput is the total network goodput (i.e., sum of the network goodput of scheduled nodes and uncoordinated nodes).

2.9 Numerical Results

2.9.1 N-PF Algorithm Performance Assessment

This subsection compares the results obtained for the N-PF algorithm and the benchmark algorithm, Proportional Fair, obtained by setting $\rho = 0$ in the N-PF algorithm. Packet length adaptation scheme is not applied, therefore both the scheduled and the uncoordinated nodes transmit packets of fixed length.

Fig. 2.7 shows the packet delivery rate for the scheduled nodes versus ρ for different number of uncoordinated nodes. From the figure it is evident that N-PF algorithm achieves up to 35% gain compared with PF algorithm in all cases. Furthermore, the PDR increases with ρ and decreases when increasing the number of uncoordinated nodes, M. The former trend is due to the fact that, for higher values of ρ, the scheduler selects the nodes with the largest value of $1/\Omega_j$ (i.e., having the largest number of neighbors, n_j), which results in minimizing collision loss probability. The latter trend is attributed to the fact that packet collisions rise when increasing M. Fig. 2.8 shows the impact of packet length on packet delivery rate. The PDR of scheduled nodes increases by decreasing packet length, because of lower collisions probability.
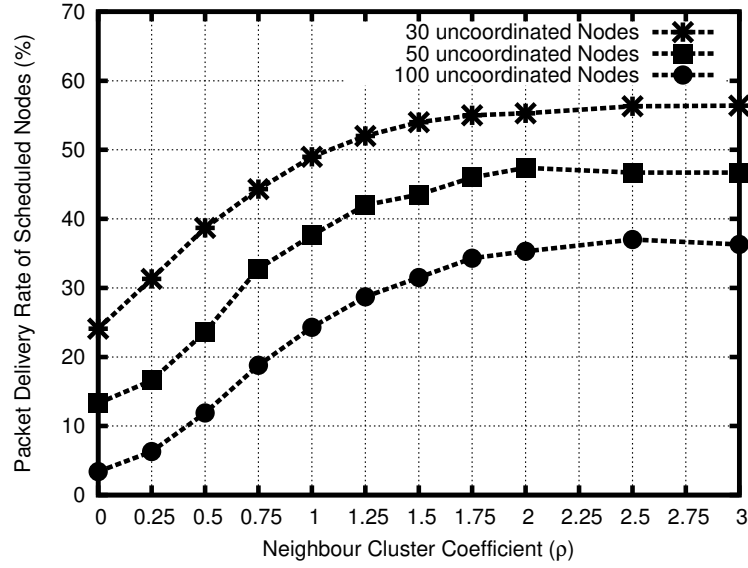
Figure 2.7: Packet delivery rate of the scheduled nodes with $K = 100$, CCA_{thr} =-85 dBm, $L = 50$ sub-slots and different values M.
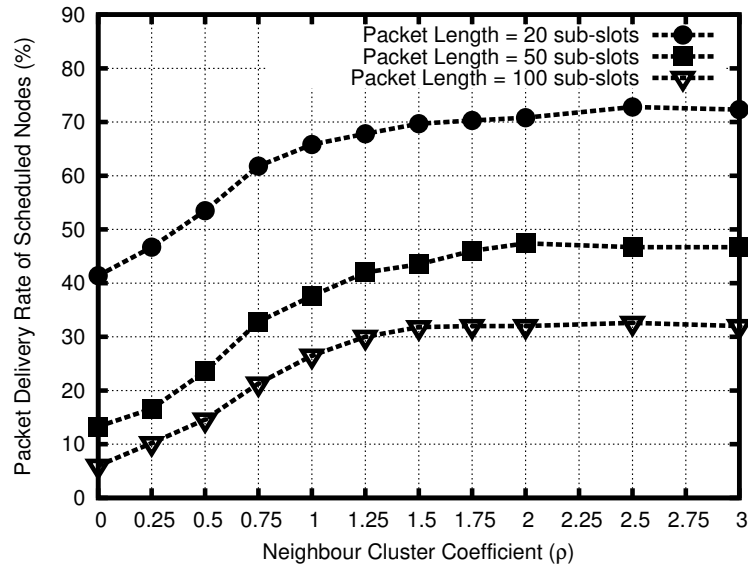
Figure 2.8: Packet delivery rate of the scheduled nodes with $K = 100$, $M = 50$, CCA_{thr} =-85 dBm, and different packet sizes.
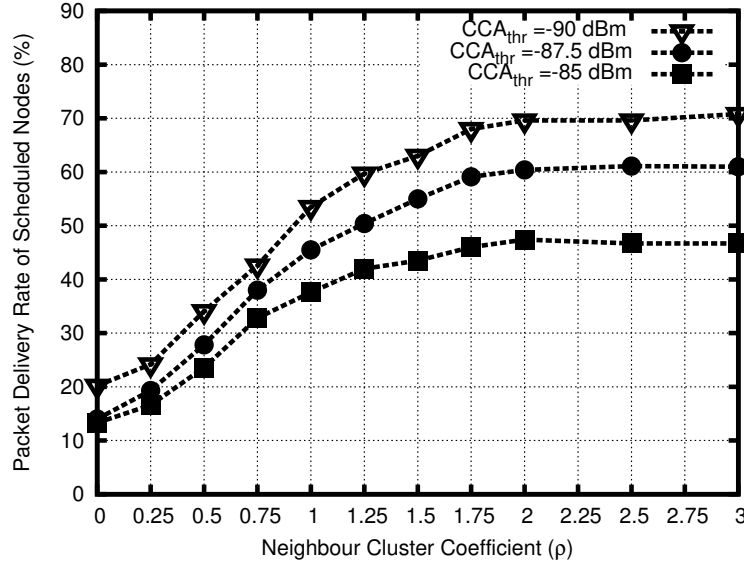
Figure 2.9: Packet delivery rate of the scheduled nodes with $K = 100$, $M = 50$ and different values of CCA_{thr}.

Figs. 2.9 and 2.10 show the impact of CSMA parameters (BE and CCA threshold) on the scheduler. As can be seen, the performance of N-PF compared to the PF algorithm improves with decreasing CCA_{thr}. For example, in the case of CCA_{thr} equal to -90 dBm the gap between N-PF and PF algorithms in terms of PDR can be up to 50%. Furthermore, as a general trend for all the cases, packet delivery rate of the scheduled nodes increases when decreasing CCA_{thr} and increasing BE because: a) decreasing CCA_{thr} results in lower average number of hidden neighbors per scheduled node, b) increasing BE spreads the channel access time for the uncoordinated nodes in a larger time window, hence reduces losses.
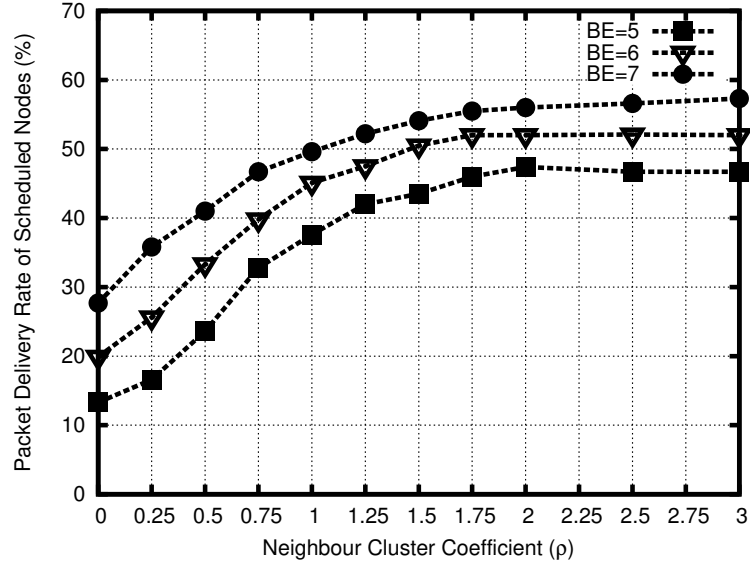
Figure 2.10: Packet delivery rate of the scheduled nodes with $K = 100$, $M = 50$, CCA_{thr} =-85 dBm and different values of BE.

2.9.2 Results With CA and DUD Schemes

In this subsection results were obtained by applying CA and DUD packet length adaptation schemes together with the N-PF resource allocation algorithm.

Fig. 2.11 shows the network goodput for scheduled and uncoordinated nodes when varying ρ, for different values of CCA_{thr}. This metric increases with ρ for scheduled nodes, demonstrating that the term $1/\Omega_j(t)$ in eq. (8) strongly impacts the goodput. On the other hand, when increasing ρ, larger priority is given to scheduled nodes having more neighbors, resulting in having more uncoordinated nodes refrained from accessing the channel. Therefore, NG for uncoordinated nodes decreases with ρ. This is demonstrated also in Fig. 2.13, where the blocking rate for uncoordinated nodes is shown as a function of ρ: as expected BR increases with ρ.
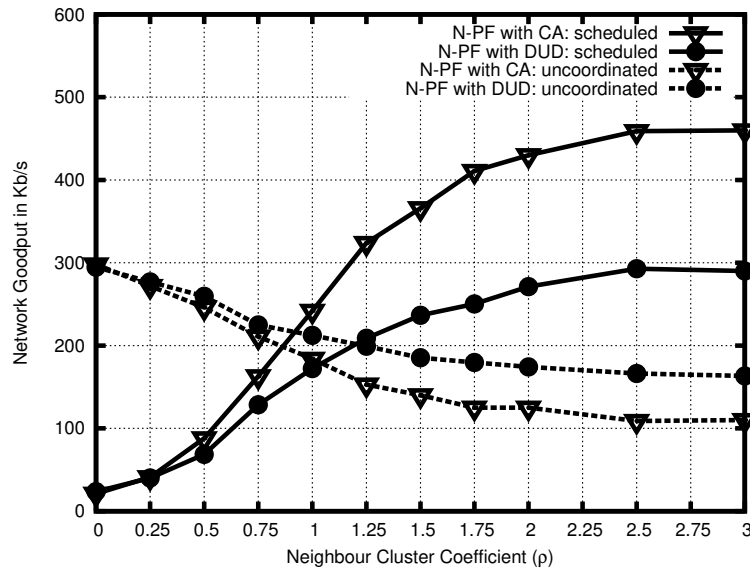
Figure 2.11: Network goodput with CA and DUD algorithms, for $K = 100$, $M = 100$ and $CCA_{thr} =$-90 dBm.
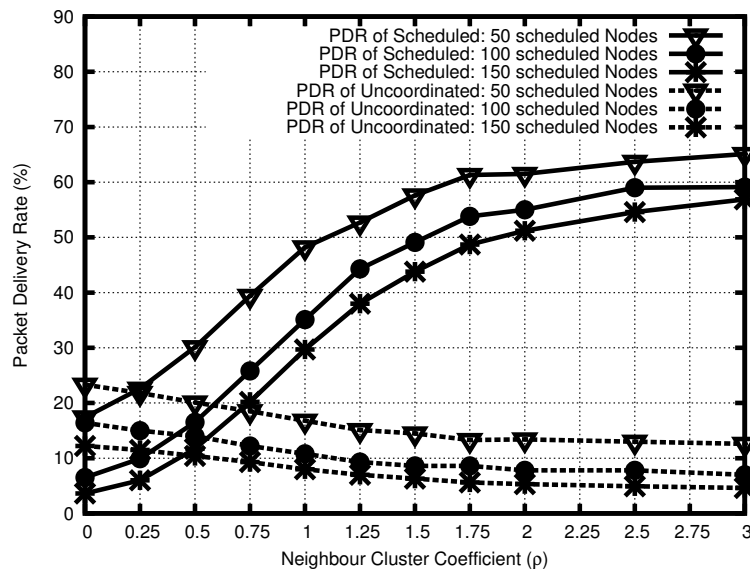
Figure 2.12: Packet delivery rate in the case of N-PF with CA algorithm, for $K = 100$, $CCA_{thr} =$-90 dBm, and different values of M.

With reference to the comparison between CA and DUD packet length algorithms, in Fig. 2.11 It seen that CA always improves the goodput for scheduled nodes, because of the effect of transmitting longer packets. On the other hand, CA worsens performance for uncoordinated nodes, since it gives more priority in the access to the channel (i.e., longer packets) to scheduled nodes. As shown in Fig. 2.13, in fact, the blocking rate for uncoordinated nodes increases when using CA.

Similar results/behaviours can be seen also in Fig. 2.12 showing the effects of using N-PF and CA on the packet delivery rate: PDR for scheduled nodes increases with ρ, while it decreases for uncoordinated nodes. In the figure we can also see that, as expected, the packet delivery rate of both, scheduled and uncoordinated nodes, decreases with increasing the number of uncoordinated nodes, due to larger collision rate. Fig. 2.11 also shows the notable improvement of the goodput that can be reached when using N-PF w.r.t. to the case of PF ($\rho = 0$), when CA is used; this improvement is much larger than the worsening obtained for uncoordinated nodes. This is demonstrated also in Fig. 2.14, where the overall channel utilization index as a function of ρ is shown. As can be seen, both the use of N-PF and CA improve the channel utilization.

Regarding the impact of the CCA_{thr}, in Fig. 2.14 it is shown that the channel utilization increase by decreasing the CCA threshold, since scheduled nodes may 'hear' more uncoordinated nodes. This results again in increasing the blocking rate for uncoordinated node, shown in Fig. 2.13.

Finally, Fig. 2.15 reports the Jain index for N-PF with CA and DUD algorithms as a function of ρ, for different values of the CCA threshold. In all cases there exists an optimum value of ρ maximizing the Jain index. In fact, when ρ is low, the
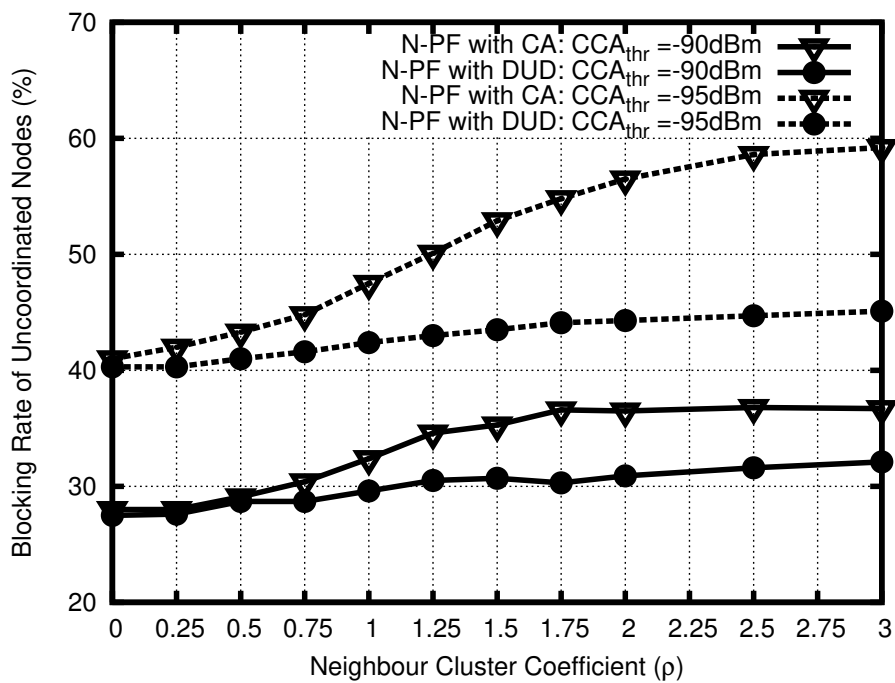
Figure 2.13: Blocking rate of uncoordinated nodes with CA and DUD algorithms, for $K = 100$, $M = 100$ and different values of CCA_{thr}.
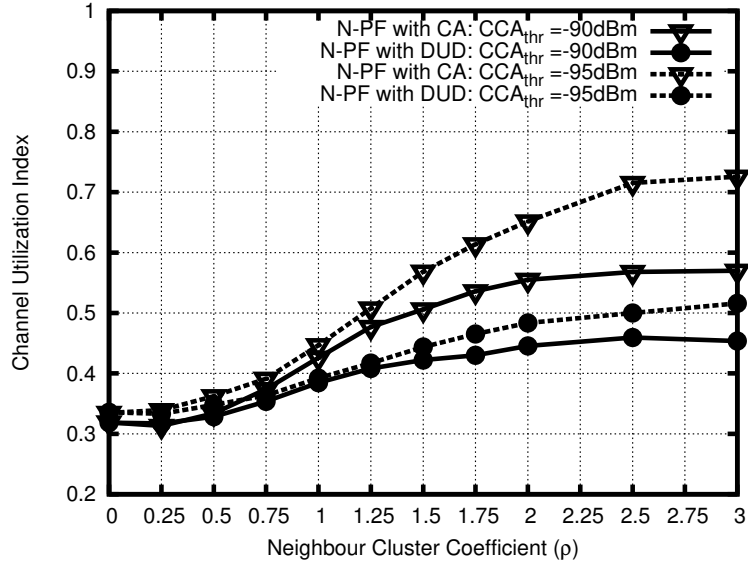
Figure 2.14: Channel utilization index with CA and DUD algorithms, for $K = 100$, $M = 100$ and different values of CCA_{thr}.

scheduling metric is mainly affected by the first term of eq. (8), while the term $1/\Omega_j$ only introduces an additional randomness into the scheduling algorithm, resulting in increasing fairness when ρ increases. When ρ becomes large, the impact of the second term in eq. (8) is predominant and a further increasing of ρ results in lower Jain index, since the N-PF algorithm tends to unfairly treat nodes. N-PF, in fact, gives more priority to scheduled nodes with a larger set of neighbors. Moreover, the optimal value of Jain index shifts to the right with decreasing CCA_{thr}: when decreasing the CCA threshold, the sensing area of nodes increases, reducing border effects, and resulting in larger fairness. Moreover, we can note that when ρ is lower than the optimum value, CA is slightly better than DUD, due to the randomness introduced by CA algorithm on N-PF algorithm. While for large values of ρ the trend reverses and N-PF with DUD outperforms CA, because CA introduces additional disparity in
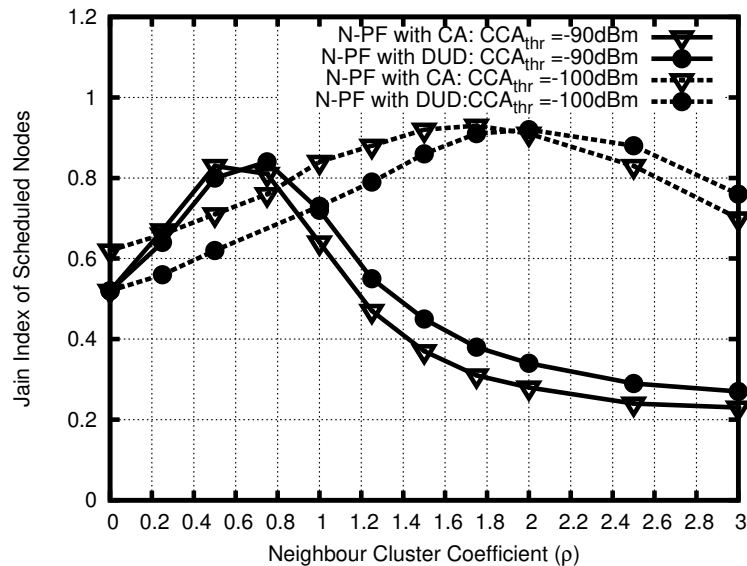
Figure 2.15: Jain Index of the scheduled nodes with CA and DUD algorithms, for $K = 100$, $M = 100$ and different values of CCA_{thr}.

resource allocation.

Finally, note that by properly setting the value of ρ N-PF allows the improvement also of fairness w.r.t. the PF algorithm.

2.10 Conclusions

This chapter presented a novel centralized scheduling algorithm for resource assignment in a scenario where scheduled nodes coexist on the same pool of radio resources with uncoordinated nodes. Through simulations it has been demonstrated that, the N-PF algorithm outperforms the benchmark algorithm, that is proportional fair, in terms of network goodput, packet delivery rate and channel utilization, without compromising fairness. Moreover, channel-aware packet length adaptation algorithm,

which allows to further improve the network goodput when compared to the discrete uniform distribution packet length selection scheme has been proposed and evaluated. Finally, the effect of different CSMA parameters, as the backoff exponent and the CCA threshold have been discussed. Results show that the performance improvement of N-PF algorithm in terms of Jain index and channel utilization, compared to PF algorithm, increases with decreasing CCA_{thr}. In conclusion, by properly setting ρ, N-PF with CA can achieve, with respect to PF with DUD, a gain of 800% in terms of network goodput for scheduled nodes, 133% in terms of channel utilization and 50% in terms of Jain Index.

Chapter 3

Multi-Hop Network Solution

Chapter 2 dealt with solutions for single-hop coexistence network. This chapter deals with coexistence of heterogeneous networks where the scheduled nodes communicate with BS in multi-hop fashion. The chapter is focused on the design of both routing and scheduling protocols, for such scenario.

3.1   Introduction

Multi-hopping technique provides several advantages when addressing coexistence of networks. First, if no power control is applied, short-hop communications can result in higher packet capture success probability in presence of interference resulting other networks. This is due to the fact that, when the transmit power of nodes is fixed, the received power of the useful link, and hence Signal-to-Interference Ratio (SIR), is higher in the case of short-range communications than in the case long-range communications because of reduced path-loss. Second, the technique allows for extension of network coverage so as to allow users far away from the BS or sink

to be connected. Thirdly, when scheduled users are configured to communicate in short-hops without applying power control, the user density could be increased. This is because short-range links can tolerate more interference than long-range links. Finally, if power control is applied and the scheduled users configured to transmit in short hops, the performance of CSMA users can be improved due to the effect of reduced interference, and this enhances fair and friendly coexistence.

As in the case of Chapter 2, the chapter addresses a scenario where scheduled nodes coexist on the same spectrum with CSMA-based nodes generating interference. Different from Chapter 2, this Chapter is multi-hop communications for the scheduled nodes is included. The aim is to design scheduling and routing protocols for the scheduled nodes accounting for the presence of uncoordinated nodes. To this aim, a novel routing scheme, based on a novel link cost metric, hereafter denoted as *Coexistence-Aware (CoA) metric* is proposed. CoA is designed accounting for both, the number of potential interferers around the receiver and the power received over the link. The best path is computed by searching for the path which is characterised by the minimum total cost. The output of the routing scheme is a set of paths which serves as input to the Multi-Link Proportional Fair (MLPF) scheduling scheme, which assigns time slots to nodes considering the bottle-neck links (i.e., links with the lowest possible achievable rates according to Shannon formula). The MLPF is a modified version of the algorithm presented in [59], where the level in the tree of the node (i.e., its distance in number of hops to the BS (root of the tree)) to be scheduled is taken into account as part of the aggregate scheduling metric. For the benchmark scheduler, the algorithm presented in [59] is considered while for the benchmark routing scheme the Dijkstra's algorithm with Received Power Aware (RPA) metric is considered.

3.2 Related Literature

In the current state of art studies on coexistence of heterogeneous networks have focused on single-hop networks and especially the design of MAC protocols. Designing routing protocols for heterogeneous networks is related to the design of interference-aware routing. Despite some initial efforts, these protocols are quite challenging to design because it is not yet clearly understood how to best capture the effects of interference in the protocol design. Authors in [60] analytically model the effect of interference on data reception probability and apply the model in the design of interference-aware routing protocol. [61] studies interference-aware routing in energy constrained cognitive ad hoc radio networks. The authors consider the area of overlap between coverage areas of the secondary and primary users as a routing metric. In [62] Authors propose propose interference aware routing metric for WMN. The proposed metric takes into account both inter-channel and intra-channel interference. [63] Studies interference-aware multi-hop path selection for D2D in cellular networks.

To the best my knowledge, there is no existing works in literature which has addressed the coexistence problem between TDM and CSMA nodes with routing protocol design.

3.3 Contribution and Structure of the Chapter

This chapter contributes to the literature of scheduling and routing protocols for heterogeneous coexistence scenarios. The contributions of the chapter can be summarised as follows:

- A novel path selection metric known as Coexistence-Aware metric is proposed and its performance evaluated. The metric aims at limiting the interference caused by uncoordinated nodes on the scheduled nodes, when considering an heterogeneous scenario where nodes are sharing the same spectrum.

- Multi-Link Proportional Fair scheduling scheme is proposed and its performance evaluated. The scheme relies on the output of Dijkstra's algorithm to assign resources to scheduled nodes, accounting for the traffic generated by nodes and their level in the tree.

The rest of the chapter is organised as follows: Section 3.4 describes the system model, Section 3.5 describes the benchmark and proposed routing schemes, Section 3.6 describes the scheduling algorithms, Section 3.7 describes the simulator setup and performance metrics, Section 3.8 provides numerical results and discussions, and finally Section 3.9 provides conclusions of the chapter.

3.4   System Model

3.4.1   Reference Scenario

The single hop scenario reported in Chapter 2 under System Model section, is extended to a multi-hop scenario as shown in Fig. 3.1. In this case, the scheduled nodes communicate in multiple hops to reach the BS.

The following definitions are given.

Definition 1 (*Average Received Powers Matrix*)**.** We define as $\underline{\underline{P}}_R = [P_{R_{i,j}}]_{i,j \in \{0,..,N\}}$ the $(N + 1) \times (N + 1)$ matrix, where $P_{R_{i,j}}$ is the average power received by node
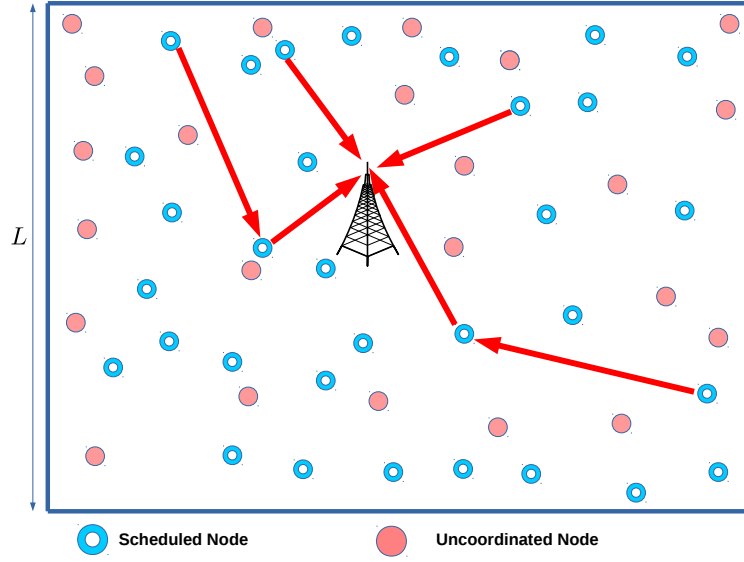
Figure 3.1: Heterogeneous multi-hop scenario.

j when node i is transmitting and considering the N scheduled nodes and the BS. $P_{R_{i,j}} = 0$ for $i = j$. Power values are averaged over fading effects.

It is assumed that the BS is centrally aware of the Average Received Powers Matrix.

Definition 2 (*Connectivity Graph*)**.** We define the directed weighted graph representing the network, also known as *Connectivity Graph*, as $G = (V, E)$, where $V = \{v_0, v_1, .., v_N\}$ is the set of vertices of the graph, corresponding to the N nodes in the network plus the BS; E is the set of edges, $e_{i,j}$, joining vertex i to vertex j. An edge from i to j ($v_i \rightarrow v_j$) exists if $SNR_{i,j} \geq \epsilon$, where $SNR_{i,j} = \frac{P_{R_{i,j}}}{2N_0 R_b}$, N_0 is the noise bilateral power spectral density, R_b is the bit rate and ϵ is the minimum requested signal-to-noise ratio. The BS is denoted as v_0.

Definition 3 (*Adjacency Matrix of the Connectivity Graph*)**.** We define as $\underline{\underline{W}} =$

$[w_{i,j}]_{i,j \in \{0,..,N\}}$ the $(N+1) \times (N+1)$ matrix, having as elements the weights of the links connecting each couple of vertexes i, j. These weights will be properly designed (see below).

3.4.2   Traffic and Packet Capture Models

All nodes generate packets according to a Poisson arrival process with arrival rate λ [bytes/frame] and each packet occupy g sub-slots as shown in Fig. 2.5. The channel model is as reported in chapter 2 under Sec. 2.5.

We assume that a packet is correctly captured at the receiver if $SNR_{i,j} \geq \epsilon$ and $SIR_{i,j} \geq \alpha$. Where α is the protection ratio and $SIR_{i,j}$ is the signal-to-interference ratio, given by:

$$SIR_{i,j} = \frac{P_{R_{i,j}}}{\sum_{k \in (all\ interferers)} P_{R_{k,j}}} \tag{3.4.1}$$

where k is an uncoordinated node interfering on the link i, j.

We account for the fact that if the transmission of a node in the tree does not succeed, all packets generated/forwarded by the children of that node will be lost.

3.4.3   CSMA/CA Protocol

The uncoordinated nodes implement the CSMA/CAprotocol described in chapter 2 under Section 2.5.

3.5   Routing Protocols

The following definitions are given.

Definition 4 (*Paths*). We define as $\underline{\underline{p}}$ the paths matrix, where the i-th line, $\underline{\underline{p}}[i]$ represents the path of node i (i.e., the set of nodes connecting i with the BS).

Definition 5 (*Paths Costs*). We define as $\underline{h} = [h_i]_{i \in \{0,..,N\}}$ the $(N+1)$-element vector including the total cost of the path connecting node i to the tree root. The cost of a path is defined as the sum of the weights of all links in the path. The path cost for the BS (i.e., the root of the tree) is equal to zero.

Therefore, the routing problem consists in the following. Given the connectivity graph, $G = (V, E)$, the related adjacency matrix $\underline{\underline{W}}$ and the vertex representing the BS, find out the path matrix, $\underline{\underline{p}}$, which minimizes the path costs.

To this aim the Dijkstra's algorithm is considered, a very well-known solution for deriving paths, between a set of nodes and a single-destination (the sink in this case), characterised by the smallest sum of link weights [64]. As is well known, the algorithm results in a tree, rooted at the BS, that is optimal, since minimises the sum of weights along the paths from any node to the root. Therefore, the routing problem consists in a proper design of the links weights, possibly accounting for the interference generated by the uncoordinated nodes.

3.5.1 Benchmark Routing Scheme: Received Power-Aware (RPA)

The benchmark is a linear and monotonically decreasing link cost function provided in [65] and the Dijkstra's algorithm. The authors studied the scheme in centralized wireless sensor networks. The motivation for chosing the scheme was due to the limited literature on routing protocols for heterogeneous coexistence, and easy implementation of the algorithm due to ready availability of the source. According to the

algorithm the link cost function is given as

$$w_{i,j_{RPA}} = w_{max} - \frac{(P_{R_{i,j}} - P_{R_{min}}) \cdot (w_{max} - w_{min})}{(P_{R_{max}} - P_{R_{min}})} \quad (3.5.1)$$

where the maximum and the minimum link weights, w_{max} and w_{min} respectively, are to be set [65]. On the other hand, $P_{R_{min}} = \min_{i,j} P_{R_{i,j}}$ and $P_{R_{max}} = \max_{i,j} P_{R_{i,j}}$ are the minimum and maximum values, respectively, of the elements of the matrix $\underline{\underline{P}}_R$ in dBm units.

The Dijkstra's algorithm takes as an input the adjacency matrix $\underline{\underline{W}}$ whose entries are computed according to equation (3.5.1), and then outputs the minimum cost paths $\underline{\underline{p}}$, composed of a of the set of links connecting all the nodes to the BS.

3.5.2 Proposed Routing Scheme: Coexistence-Aware (CoA)

The proposed scheme attempts to address the problem of interference in an heterogeneous coexistence scenario described in this thesis. Each scheduled link $e_{i,j}$ is characterised by a set of uncoordinated nodes, $U_{i,j}$, which are not generating harmful interference, that is they may transmit together with v_i without causing harmful interference. Therefore, an uncoordinated node, m, will belong to $U_{i,j}$ if $P_{R_{i,j}}/P_{R_{m,j}} \geq \alpha$.

For $M > 0$, we define a new link cost $w_{i,j_{CoA}}$, based on number of potential interferers on the link as

$$w_{i,j_{CoA}} = w_{i,j_{RPA}} \cdot \left(\left| \log_{10} \frac{|U_{i,j}|}{M} \right| \right)^{\rho}, \quad (3.5.2)$$

where $|U_{i,j}|$ is the size of $U_{i,j}$ and ρ is an optimization parameter to trade-off the average number of hops in the network and packet delivery rate.

Therefore, in absence of uncoordinated nodes or $\rho = 0$ the coexistence aware metric switches to the benchmark metric, $w_{i,j_{RPA}}$. When ρ increases the routing

protocol tends to favour routes with few potential interferers.

3.6   Scheduling Algorithm

Once the routing stage has been completed and the paths matrix has been found, the problem of resources assignment is addressed considering the Multi-Link Proportional Fair (MLPF) algorithm.

In a single hop network, the scheduler selects the set of users with the best relative metric, $s_i(t) = \frac{R_i(t)}{\underline{R}_i(t)}$. Where $R_i(t)$ and $\underline{R}_i(t)$ are the current achievable rate and the past average rate of user i at scheduling time instant t, respectively. In this chapter, we compute $R_i(t)$ according to the normalised Shannon formula given as $R_i(t) = \log_2(1 + SNR_{i,j})$, where j is the parent of i in the tree (i.e., $j = \underline{p}[i, i+1]$). On the other hand, $\underline{R}_i(t)$ is computed as an exponential moving time average and it is given as by equation (2.6.1). The motivation for chosing proportional fair scheduling in this thesis is because the algorithm has already been proved in literature to be throughput optimal [66].

To extend the proportional fair scheme described above to the case of multi-hop the approach presented in [59] is modified. At each scheduling instant t, the scheduler assigns resources to nodes considering the path matrix $\underline{\underline{p}}$ and the available resources. If node i is selected by the scheduler at time instant t as the next user to be scheduled, all links on the path from i to the BS (i.e., $\underline{p}[i]$), are first assigned time slots, before another user k on a different path is scheduled (refer to Fig. 3.2). Therefore, this scheme considers a path-by-path scheduling.

Moreover, in order to take into account the fact that nodes nearer to the BS may be requested to transmit more packets (they have to forward packets coming from
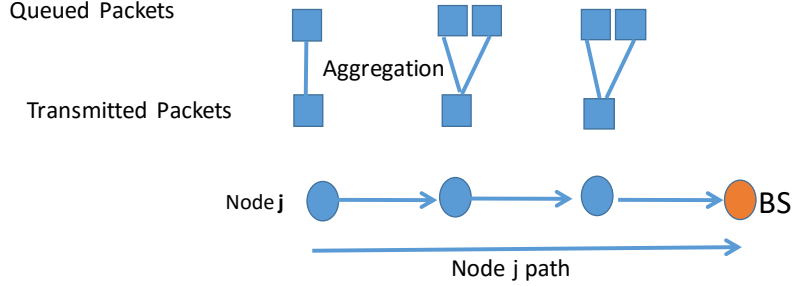
Figure 3.2: Data aggregation strategy: an example with $\eta = 3$ packets.

their children in the tree), the scheduling metric is modified as follows:

$$s_i(t) = \min_{i \in \underline{p}[i]} \frac{R_i(t)}{\underline{R}_i(t)} \cdot \frac{1}{l^\xi} \tag{3.6.1}$$

where l represents the level at which the node is (at $l = 0$ we have the BS, at $l = 1$ we have the children of the BS, etc.), and ξ is a design parameter to be properly set. The above equation accounts for the fact that in the case of multi-hop the scheduling metric of a path corresponds to that of the bottleneck link of the path $\underline{p}[i]$ at time instant t.

Note that by increasing ξ, we give more priority in the channel access to those nodes nearer to the BS.

Finally, we assume that each scheduled node in the tree may aggregate up to η packets, therefore a node may compress up to η packets into g sub-slots, without loosing information. In case the queue contains more than η packets, more resources should be assigned to the node. Note that the case $\eta = 1$ corresponds to the absence of data aggregation. The aggregation strategy is shown also in Figure 3.2.

3.7 Simulation Environment

3.7.1 Simulator and Parameters

For performance evaluation we developed a C++ simulator implementing our system model, routing and scheduling algorithms. 200 scheduled nodes and 100 uncoordinated are randomly and uniformly distributed in the square cell. The channel is divided into frames with each frame containing 10 slots. Each slot is further subdivided in 200 sub-slots. All nodes generate traffic according to Poisson's arrival process at a rate of 500 bytes per frame (1 packet per frame). For the benchmark scheme the parameters $w_{max} = 100$ and $w_{min} = 1$ are adopted as given by authors in [65]. Other parameters are specified in Tab. 3.1. Results are obtained by averaging over 100 different scenarios, where a single scenario is characterized by different positions of nodes and fading samples.

3.7.2 Performance metrics

1. **Average number of Hops**: This mean number of hops required to deliver packet from the source to the BS.

2. **Packet Delivery Rate**: this is the fraction of the transmitted packets which is correctly received at the BS, and expressed as %.

3. **Throughput**, given by

$$Throughput = \frac{Received\,bits\,in\,1000\,frames}{Duration\,for\,1000\,frames}$$

65

Table 3.1: Default Simulation Parameters

Parameter	Default Value
L	1000 m
N	200
M	100
P_T	20 dBm
β	0.5
k_0	41 dB
k_1	30
λ	1 packet/frame
α	3 dB
ϵ	5 dB
BS height	20 m
NB_{max}	10
CCA_{Thr}	-90 dBm
CW	31 sub-slots
BE	5
R_b	1 Mbps
N_0	10^{-20} W/Hz
T	10
a	200
g	50
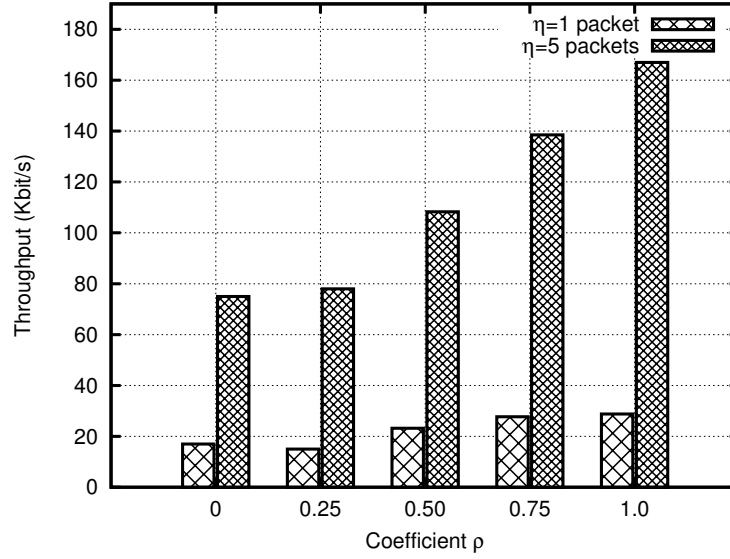
Figure 3.3: Throughput of the scheduled nodes with Packet Aggregation (η) set to 1 and 5.

4. **Jain Index (JI)**, the metric for measuring the fairness of a scheduler in resource allocation. It is given by equation (2.8.1).

3.8 Numerical Results

The performance of CoA routing metric with respect to RPA metric is reported in Figs. 3.3, 3.4, 3.5, and Tab. 3.2. The performance of the two routing metrics is compared using the MLPF scheduler, i.e., by setting the scheduler coefficient $\xi = 0$, in the equation (3.6.1). As discussed in the Sec. 3.5, the performance of the benchmark routing scheme is obtained by setting the coefficient $\rho = 0$. Fig. 3.3 reports the throughput performance of the CoA routing scheme with and without packet aggregations (η set to 1 and 5 packets respectively). As shown in the Figs.
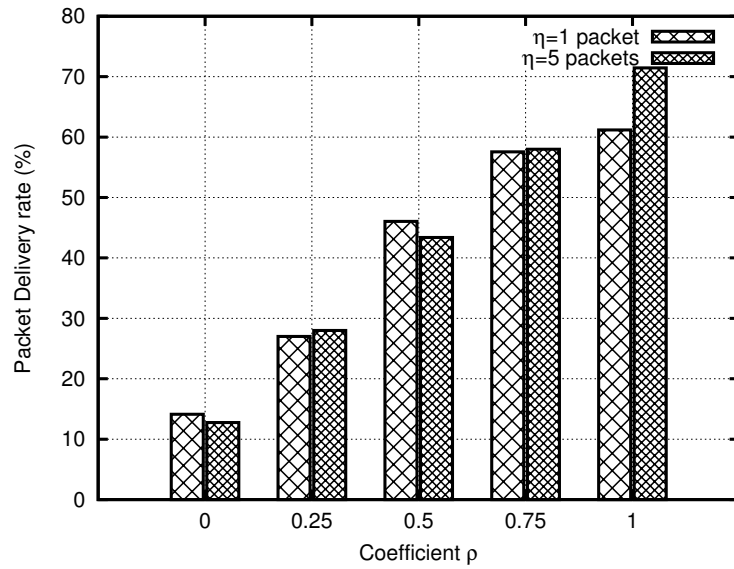
Figure 3.4: Packet delivery rate of the scheduled nodes with Packet Aggregation (η) set to 1 and 5.
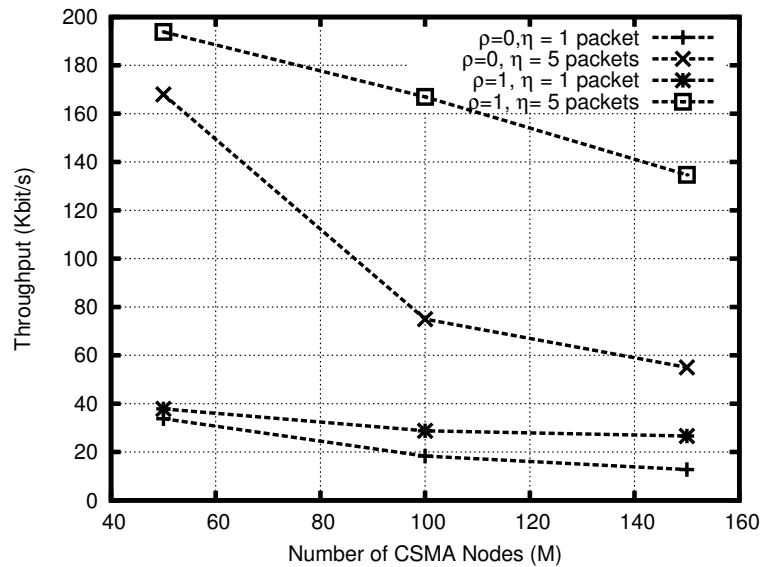
Figure 3.5: Effect of the number of uncoordinated nodes.
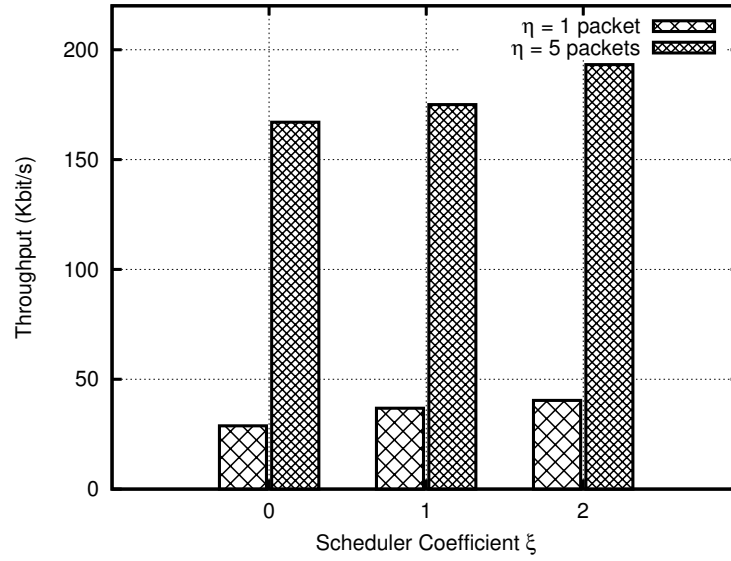
Figure 3.6: Throughput performance for different values of coefficient ξ.

Table 3.2: Average Number of Hops

Coefficient (ρ)	Hops
0	2.24
0.25	5
0.5	7.1
0.75	8.5
1	9.45

3.3 and 3.4, throughput and packet delivery rate increase with the coefficient ρ, i.e., from $\rho = 0$ (**benchmark**) up to $\rho = 1$. This is due to the fact that, as ρ raises the CoA scheme tends to favour routes with fewer number of potential interferers. Fig. 3.3 also shows an improvement in the network performance when packet aggregation is applied compared to the case when no packet aggregation is used. This trend can be attributed to the effect that, with packet aggregation the scheduled paths tend to transport more information than when no aggregation is applied. Considering the case of packet aggregation ($\eta = 5$ packets), the CoA algorithm results in throughput gain of 122.6% in respect to the benchmark routing protocol. However, these gains are achieved at a cost of increased number of hops as depicted in Tab. 3.2. In this case, number of hops is not affected by the parameter η.

Fig. 3.5 reports the effect of the number of uncoordinated nodes on the general performance of the scheduled nodes, and CoA routing scheme. From the figure, it is evident that, the throughput decreases with increasing number of uncoordinated nodes due to increased chances of collisions.

Finally, the performance of the proposed MLPF scheduler in comparison with the Benchmark MLPF scheduler is reported in Fig. 3.6. The results for the MLPF, which is the benchmark scheduler, are obtained when the scheduling coefficient $\xi = 0$. The values were obtained with the routing coefficient $\rho = 1$. As the scheduler coefficient ξ is raised from $\xi = 0$ to $\xi = 2$, the network throughput increases. This is due to the effect that the scheduler tends to favour nodes closer to the base station (i.e. those with fewer hops) and hence higher packet success probability. Considering the case with packet aggregation, the proposed scheduling algorithm results in 40.2% improvement in throughput. In general, the MLPF scheduler is very fair and the

Jain index does not vary with the routing coefficient ρ or the scheduler coefficient ξ. in all cases reported above, the Jain index was approximated to be 0.9.

3.9 Conclusion

In this chapter addressed the problem of routing and scheduling in a coexistence scenario where scheduled nodes and uncoordinated nodes use the same channel. A novel routing scheme, denoted as CoA, has been proposed and its performance evaluated. CoA takes into account the set of potential uncoordinated nodes interfering on a given scheduled node together with received power aware metric. It has been shown that CoA scheme can tuned to trade-off the achieved network throughput and the average number of hops. Furthermore, the proposed scheme is used sequentially with Multi-Link Proportional Fairness algorithm to ensure that nodes are scheduled fairly without compromising throughput. Results show that, considering the case when $M = 100$ $\xi = 0$, and $\eta = 5$ the CoA scheme can achieve up to 122.7%, and 46.7% gains in terms of throughput and packet delivery rate respectively compared to the benchmark scheme (RPA).

Part II

UAV-based beyond 5G networks

Chapter 4

IEEE 802.11s Wireless Mesh Solution for Drone-Based Monitoring Applications

This chapter is concerned with the use of mobile drones in environmental monitoring. Due to drone mobility, it relies on relays deployed on the ground for reliable connectivity. The drone, relays and the control center are equipped with IEEE 802.11s interfaces to facilitate WMN formation. The aim of this Chapter is to design routing protocols for fast, reliable and resource efficient connectivity of the drone to the control center in order to meet the end-to-end delay requirement of video applications.

4.1   Introduction

WMN consists of a set of nodes interconnected with each other via radio links forming mesh topology. This type of radio networks provide an efficient and cost effective way to deploy large communication networks and to interconnect separated heterogeneous networks [67]. Besides the low cost and high performance, WMNs can be dynamically self-organized, self-healed and self-configured, and therefore, they can be easily

deployed and maintained.WMNs can be used in wide range of applications, such as video surveillance networks, home and community broadband access networks, military applications, etc.

Driven by the need for standardization of WMN, the IEEE 802.11s standard was developed [68] to extend the coverage of IEEE 802.11 WLANs. The standard is simply an extension of the IEEE 802.11 to support mesh forming capability. The design of WMN need to address the problem of collisions and reliable network connectivity. In multi-hop networks with CSMA-based MAC, the problem of collision is larger than in the case of single-hop networks because nodes connected with multiple links are out of visibility of each other. This problem is exacerbated with increased densification of mesh nodes. To resolve collisions, the standard proposes a distributed contention-free protocol, the Mesh Coordination Function (MCF) Controlled Channel Access (MCCA), besides the contention based MAC protocol, EDCA, of the IEEE 802.11 WLANs. In respect to connectivity, the standard proposes Hybrid Wireless Mesh Protocol (HWMP) which works on top of layer 2 of the protocol stack. The protocol is designed to work in the layer 2 instead of layer 3 in order to: facilitate exchange of routing metrics between physical layer (PHY) and MAC layer [69]; and to hide the complexity of the path determination from the upper layers such that all devices are seen to be a single hop away [70]. However, in order to address diversity of applications that follow IEEE 802.11s the standard gives a provision for vendor specific routing protocols.

As shown in Fig. 4.1, the IEEE 802.11s WMN architecture consists of four main types of nodes: basic Station (STA), Mesh Point (MP), Mesh Access Point (MAP), and Mesh Portal Point (MPP). A STA is a legacy IEEE 802.11 node which can only

External Network

**Mesh Portal Point
(MPP)**

Portal
MP

Mesh Point

MP

Mesh AP

MP
AP

Mesh AP

MP
AP

STA

STA

STA

Station

STA
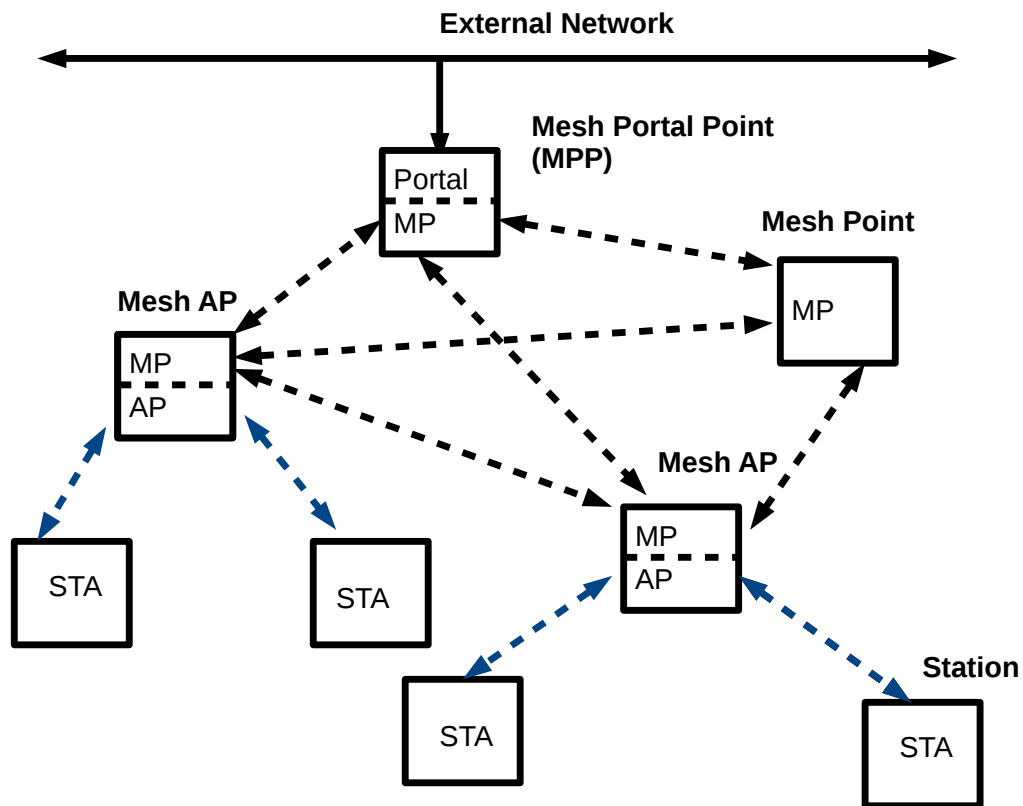
Figure 4.1: IEEE 802.11s WMN Architecture.

communicate via an Access Point (AP) and lacks capability to act as relay for other network nodes, while a MP is a network mesh node which can generate and forward its own traffic as well as relaying traffic for other mesh nodes. MAP is a MP with additional capability to serve as an AP for the IEEE 802.11 legacy nodes, and a MPP is a mesh point which serves as a gateway to the external networks. According to the standard, there are two modes of operation of a WMN: infrastructure mode, where nodes communicate through the AP, and ad-hoc mode, where nodes communicate among them without an AP relying on the principles of generic ad-hoc networks.

Chapter 4. IEEE 802.11s Wireless Mesh Solution for Drone-Based Monitoring Applications

WMN is a promising technology for many drone-based applications. This is motivated by the key features of this type of radio networks such as low cost, fast deployment and maintenance. The WMN is able to facilitate connections of a serving drone to a remote control center. Moreover, in a WMN, the drones can aid in performing other network functionalities such as acting as a data collection point, Mesh Aerial Relay (MAR), MAP, and Internet gateway. The drone could interconnect with other drones or ground nodes to form an ad hoc network. It is well known under channel modelling that, when a drone acts as a relay or a MAP it is able to cover a wide area on the ground due to the high probability of line-of-sight communication. The coverage increases with drone height up to when the optimal height is reached [30], [71]. This is very advantageous because it results in reduction of the number of nodes needed to provide reliable multi-hop connectivity, and reduction in energy consumption of the aerial nodes. However, unless well designed, WMN may not meet the needs for real-time applications such as video surveillance and hence can result to degraded performance. This is because video applications have stringent delay constraints which must be respected, but due to ineffective MAC and routing policies WMN may not guarantee these requirements.

This thesis addresses the problem of routing in IEEE 802.11s WMNs for drone-based monitoring applications. The scenario considered consists of a drone moving in a given field of interest gathering video from the environment and transmitting to a remote control center via ground mesh nodes. The ground mesh nodes are static, and therefore, the network consists of both, mobile and static components. The dynamic component consists of the drone(s) while the static component consists of ground mesh nodes. Taking advantage of this network structure, an Optimised

Hybrid Wireless Mesh protocol, denoted as O-HWMP, is designed, which ensures quick and efficient route discovery and hence low end-to-end delays suitable for video applications. Through extensive NS-3 simulations it is demonstrated that, the O-HWMP outperform the RM-AODV proposed in the standard in terms of end-to-end delay, packet success rate, radio resources utilization, and video transmission and quality metric.

4.1.1   Related Works

The research on drones is increasingly attracting interest among the scientific and industrial communities. As far as the study of drones in radio networks is concerned, the work in [29] discusses the application of drones in smart cities, their opportunities and challenges. In [72] Authors provide a survey on important issues in Unmanned Aerial Vehicles (UAVs) communication networks, emphasizing the challenges of designing routing protocols. [73] studies the problem of generating UAV communication networks for monitoring and surveillance of distant targets. In the current literature ad hoc wireless mesh architecture is believed to be the most suitable for future drone communications [72, 74].

The IEEE 802.11s standard proposes HWMP for path selection but the performance of the protocol is not well-known for many use cases because of inadequate studies. Through simulations, [75], compares the performance AODV and IEEE 802.11s HWMP. However, the authors do not consider a practical use case, and no proposal is made on how the same WMN utilize the different components of HWMP. [76] compares the performance of the reactive and proactive modes of HWMP with different types of traffic flows. Similar to [76], authors in [77] consider the two modes

of HWMP separately, and evaluate the performance of the protocol in different environments but considering only a single traffic flow. In [78] Authors provide analytical delay and throughput analysis for IEEE 802.11s WMN considering different traffic loads for mesh nodes and the HWMP. Moreover, the authors consider only reactive routing mode in the same WMN. [69] studies the performance of routing protocols in swarm of UAVs. The work considers both static and dynamic cases of UAVs and compares four protocol implementation: open80211s, BATMAN, BATMAN Advanced and OLSR. However, this study does not consider the two modes of HWMP in the same WMN. Experimental Evaluation of IEEE 802.11s path selection protocols in a mesh testbed is provided in [70] considering only the default routing component of HWMP, the Radio-Metric AODV (RM-AODV) protocol.

The work presented in this chapter of the thesis is different from the above works because none of these works consider joint operation of reactive and proactive schemes on the same WMN. Furthermore, the proposed routing protocol, O-HWMP, has never been proposed elsewhere in literature.

4.1.2 Contributions and Organisation of the Chapter

In contrast with the previous works, this thesis studies the joint operation of proactive tree-based and RM-AODV routing schemes on the same WMN with drones. Taking advantage of the structure of the network in the scenario, a new routing protocol, denoted as O-HWMP, is designed and evaluated against the standard protocol RM-AODV. According to the operation of the protocol, the output of the tree-based routing scheme provides an input to the RM-AODV protocol. This protocol design results in many advantages such as: reduced flooding of control packets in the

network, improved channel utilization, low end-to-end delay performance and reliable connectivity of the drone to the control center. The performance of the proposed protocol is benchmarked with the standard default protocol, RM-AODV. In summary there are two main contributions to the existing literature:

- A scenario where a mobile drone is used to monitor a large area and transmit video to a remote control center in multi-hop. To maintain strong connectivity between the drone and the control center routers equipped with IEEE 802.11s interfaces for WMN formation are deployed on the ground.

- Fast and resource-efficient hybrid wireless mesh protocol denoted as, O-HWMP, for video surveillance applications is designed and its performance characterised.

The rest of the chapter is organised as follows: Section 1.6 describes the system model, Section 4.2 describes the routing protocols, Section 4.3 describes numerical results and discussions and finally Section 4.4 provides conclusion.

The scenario considered is shown in Fig. 1.4, where a mobile drone is used to perform video surveillance and transmit data to a remote control center in multi-hop. There are $\mathcal{N}$ mesh points deployed in fixed positions on a square grid of side L, and a control center located at one corner of the square. The mobile drone is equipped with a mesh node to interconnect with the static network. The drone flies at a speed x [m/s], h [m] above the ground. At the application level, the drone generates video of resolution 720p. The relay nodes do not act as traffic sources but only forward traffic from neighbouring mesh nodes.

The connectivity model implemented in NS3 [79] is considered. According to this model, two nodes are connected if the transmitter-receiver distance is lower than a given transmission range otherwise they are lost. When two nodes are connected we

assume that packets are correctly received otherwise they are lost. This model is considered because it is easy to implement and is sufficient to enable characterization of the routing protocols which is the main focus of this chapter. Furthermore, all the mesh points implement IEEE 802.11a PHY and MAC. The PHY and MAC layers implement Orthogonal Frequency Division Multiplexing (OFDM) PHY with bit rates in range of $6-54$ Mbps, and Distributed Coordination Function (DCF) CSMA/CA modes respectively.

4.2 Routing Schemes

4.2.1 Benchmark Scheme: RM-AODV

The benchmark scheme considered is the RM-AODV protocol proposed by the IEEE 802.11s standard. This protocol is appropriate when MPs are mobile, and is designed to work at layer 2 of the protocol stack with MAC addresses instead of layer 3. This hides the complexity of the path determination from the upper layers such that they see all devices as a single hop away (destination nodes are seen as direct neighbours) [70], and enables easy information exchange with the PHY-layer for creating an efficient routing metric [69].

The path cost metric of the protocol reflects both the link quality (accounted by the achievable link data rate and packet error rate components) and the amount resources consumed when a given frame is transmitted over a specific link. According to the standard the link cost metric (C_l) is defined as follows:

$$C_l = \frac{(O_l + B_t/\gamma)}{(1 - e_f)} \tag{4.2.1}$$

where O_l is the channel access overhead which includes frame headers, training sequences, MAC overhead, etc. B_t is the test frame in bytes set to 1024 Bytes in the standard, γ is the link rate in Mbit/s and e_f is the test frame error/loss rate computed considering the link rate γ. The standard does not specify the way e_f metric should be computed. In this chapter, the following definition of e_f as given in NS3.

If we let S_l be the link state variable which takes value of 1 if transmission succeeded in the last time instant, and 0 otherwise. Then e_f can be defined as:

$$e_f[t] = \begin{cases} (\frac{R_C}{R_C+1}(1-a)) + a * e_f[t-1], & if \ S_l = 1 \\ (1-a) + a * e_f[t-1], & if \ S_l = 0 \end{cases} \tag{4.2.2}$$

where R_C is the retry counter which is incremented every time transmissions of given node fails due PHY or MAC issues, and a defined in the range: $0 < a < 1$, is an exponential weighting function given as:

$$a = \exp\left(\frac{L_T[t] - C_T[t]}{M_T}\right) \tag{4.2.3}$$

L_T $[\mu s]$ is the last time instant e_f was computed i.e., $[t-1]$. C_T $[\mu s]$ is the current time instant, and M_T $[\mu s]$ is the memory time which indicates the amount of memory needed for the calculation.

The path cost is the sum of metrics values for all links belonging to the path. RM-AODV chooses the shortest path from a source node to the destination node i.e., the path with the minimum cost.

4.2.2 Proposed Scheme: O-HWMP

Since the scenario has both dynamic (drone) and static (ground relays and control center) sub-components, reactive and proactive routing schemes are designed to work

in composite in order to achieve better network performance in terms of connectivity, delay and radio resources utilization. When RM-AODV is used exclusively in the network, it results in excessive delays and inefficient utilization of resources. On the other hand, proactive tree-based routing without the reactive component can result to lose of network connectivity and utilization of weak links as a consequence of the drone mobility. Therefore, none of the two schemes can work exclusively in a satisfactory manner.

In the proposed design, the proactive tree-based routing scheme is applied on the ground relays (MPs) and the control center, while the reactive routing is initiated by the mobile mesh node. The control center acts as the root node of the tree, and through the broadcast of proactive Path Request (PREQ) messages the relay mesh nodes are able to maintain updated paths to the root. The reactive routing scheme is used to find the shortest path from drone to the CC taking advantage of the existing tree topology for the static component of the network. Therefore, the reactive routing scheme depends on the output of the proactive tree-based routing. To establish a path from the source (drone) to the control center, the source broadcasts a PREQ message to all its direct neighbours (relays and control center). On receiving PREQ message, all the MPs with a valid path to the control center respond with a unicast PREP message containing cumulative radio-aware routing metric (C_{rm}). On receiving the PREP message from the MP i, the source computes the path cost (P_{c_i}) as:

$$P_{c_i} = C_{rm_i} + C_{l_i} \qquad (4.2.4)$$

where i is the node index of the MPs including the control center node, P_{c_i} is the total path cost of the route from the drone to the control center through the neighbour MP i, C_{rm_i} is the cumulative path cost from the MP i to the control center, and C_{l_i} is cost

of the link between the drone and MP i and is computed according to the equation (4.2.1). The source compares all values of P_{c_i} and selects the route with minimum value. The best path is maintained by the drone until it almost loses connectivity. Therefore with respect to the benchmark scheme, the O-HWMP is different in the following ways:

- The O-HWMP considers both proactive tree based routing and reactive RM-AODV jointly on the same mesh network such that the output of the proactive scheme forms an input to the reactive scheme. This design helps to achieve quick path discovery and hence reduces delay and wastage of radio resources while maintaining the best paths.

- All the relay nodes which receive PREQ messages from the drone and with valid paths to the destination sent back unicast Path Reply (PREP) messages with cumulative path cost to the control center.

4.3   Numerical Results and Discussions

4.3.1   Simulator setup

The simulated scenario consist of 16 fixed mesh nodes and a single source drone. The nodes are arranged on a square grid spaced 50 m apart both horizontally and vertically. The drone flies 30 m above the ground at speed of 5 m/s diagonally from one corner of the square to the other as shown in Fig. 1.4. When a path between the drone and the control center has been established, the drone starts to transmit a higher definition video ($720p$) encoded in MP4 format with a frame rate of 24 fps.The

video consists of 1253 frames of variable sizes and lasts for 52 seconds. The frames
are fragmented into packets of maximum size of 1024 bytes to allow processing at IP
layer.

Initial values for the computation of $e_f[t]$ metric are set as follows: $L_T[0] = 0$s,
$C_T[0] = 0$s and $M_T[0] = 1$s

4.3.2   Performance metrics

1. Average Delay [ms]: the average end-to-end delay measured considering the
   application layer of the drone (source) and control center (client). It is computed
   as the mean of the end-to-end delays of all received packets.

2. Packet Success Rate [%]: is the ratio of the packet received by the control center
   to the total packets transmitted by the drone expressed as a %.

3. Average Window Delay [ms]: this metric shows the evolution of average delay
   in time as the drone moves from the control center to the extreme end of the
   monitored area. The average delay is evaluated with a fixed window of 2000
   frames, i.e., for every 2000 frames received the average delay is computed and
   the window is reset.

4. Routing Overhead: this metric is measured by summing all management packets
   of the routing protocol for all the nodes in the network. The management frames
   include PREQ, PREP, and Path Error (PERR).

Table 4.1: Comparing Protocol Overhead and PSNR

Protocol	Overhead [Bytes]	PSNR [dB]
RM-AODV	190497.3	19.52
O-HWMP	8099.2	24.49

5. Peak-Signal-to-Noise-Ratio (PSNR)[dB] [80]: this metric is computed with El-vavid tools considering the input and the output raw videos. It is given by

$$PSNR = 20.\log\left(\frac{MAX_I}{\sqrt{MSE}}\right) \tag{4.3.1}$$

where MAX_I is the maximum possible pixel value of the image (equal to 255), and MSE is the mean square error given as:

$$MSE = \frac{1}{NM}\sum_{m=1}^{M-1}\sum_{n=1}^{N-1}\left[I(i,j) - K(i,j)\right]^2 \tag{4.3.2}$$

where I and K are the original and compressed images respectively of dimensions $M \times N$.

4.3.3 Numerical Results

Figs. 4.2-4.4 show the performance of the IEEE 802.11s RM-AODV and O-HWMP protocols. Fig. 4.2 compares the protocols in terms of average delay performance. As a general trend, the average delay decreases with increase in transmission range. This effect is due to the fact that the number of hops and protocol processing overhead decrease with raising the transmission range. Comparing the two schemes, O-HWMP outperforms the RM-AODV protocol in all cases of transmission ranges and this is because O-HWMP takes advantage of the proactive tree-routing component to speed up path discovery.
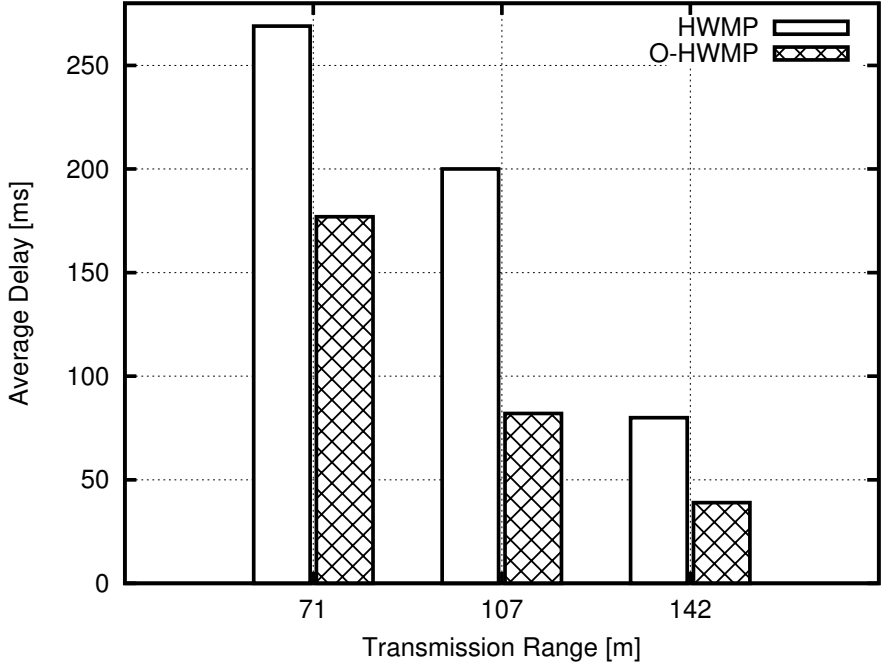
Figure 4.2: Average packet delay .
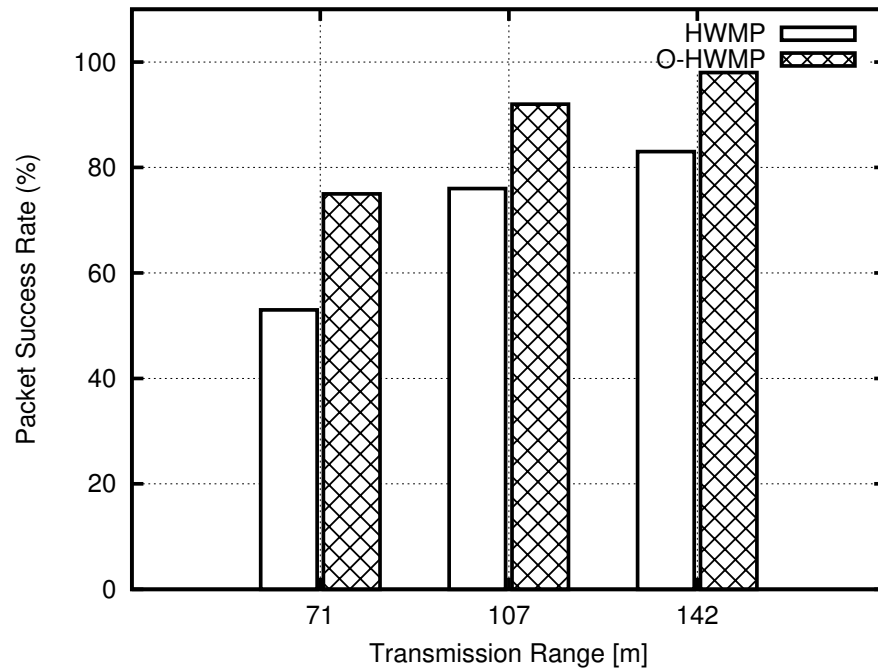
Figure 4.3: Packet success rate.
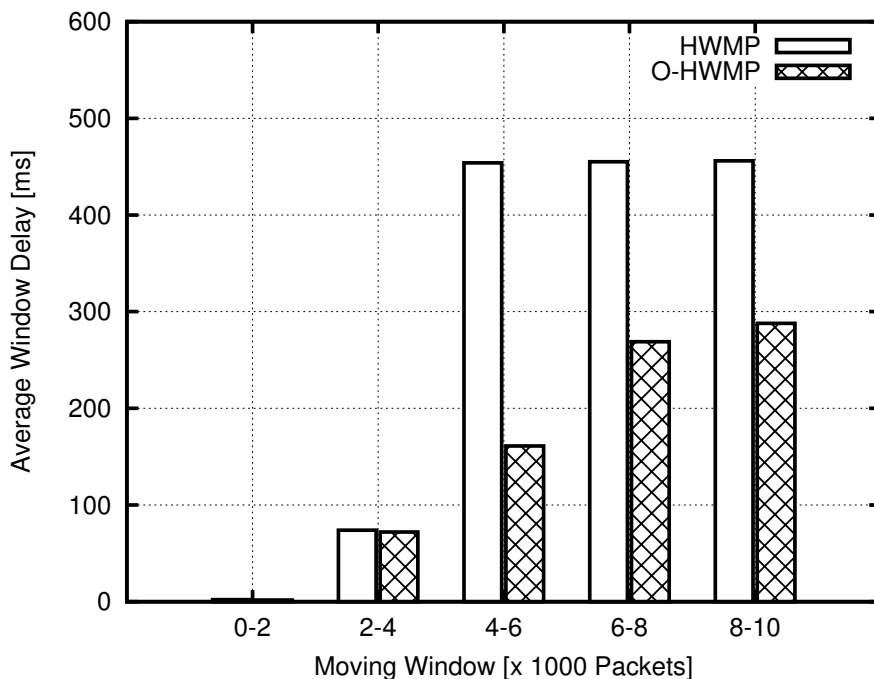
Figure 4.4: Average Window Delay based on Fixed Window of Received Packets (2000 packets)

Fig. 4.3 reports the performance of the protocols in terms of packet success rate. In both schemes, packet success rate raises with increasing transmission range. This is due to the fact that the probability of packet loss increases with increase in number of hops traversed by a packet before reaching the receiver. With respect to RM-AODV, the O-HWMP results 22%, 16% and 15% gain for 71 m, 107 m, and 141 m transmission ranges respectively. The improvement in packet delivery rate is because of lower routing overhead for O-HWMP. Fig. 4.4 shows the evolution of delay with respect to a fixed moving time window. The window is set considering received packets and it is fixed to 2000 packets. In the figure, the performance of both protocols is evaluated considering transmission range value of 71 m, therefore, in average packets

have to traverse a number of hops to reach the control center. As shown in the figure, the average delay in the first and the second window is relatively small compared to other windows. This effect could be attributed to the close proximity of the drone to CC. Similar to the average delay performance, the O-HWMP outperforms RM-AODV in terms of average window delay.

Tab. 4.1 compares the performance of the routing schemes in terms of routing overhead and PSNR metrics. In both cases the results are obtained when transmission range is set to 71 m. According to the table O-HWMP results in 95.7% reduction in routing overhead with respect to RM-AODV. This is because the O-HWMP protocol floods less management packets in the network compared to RM-AODV. On the other hand O-HWMP results 25.5% gain in PSNR compared to RM-AODV.

4.4 Conclusion

The chapter presents a scenario where a mobile drone is used to monitor a large area on the ground and convey video information to a remote control center in multi-hop. To maintain strong connectivity between the drone and the control center routers are deployed on fixed positions on the ground. Furthermore, a novel hybrid routing scheme, denoted as O-HWMP, has been designed and its performance evaluated. O-HWMP outperforms the IEEE 802.11s RM-AODV protocol in terms of packet success rate, average delay, protocol overhead, and received video quality measure using PSNR metric.

Chapter 5

Joint Routing and Scheduling for Multi-Hop radio networks with drones

5.1 Introduction

Similar to Chapter 4, this chapter studies an application scenario for drones in environmental monitoring. The scenario consists of a mobile drone which is used to monitor events of interest on a large area, and to transmit data to a remote control center via static relays placed on the ground in multi-hop. The aim of the work is to design high capacity and low delay arouting and scheduling protocol appropriate for the scenario. The problem of routing and scheduling protocol is addressed with BP and FlashLinQ schemes. In a multi-commodity (multi-flow) network, the BP decides on each slot the flows to be sent on each of the links present in the network. For the link rate computation the algorithm requires a scheduler to decide on a maximal subset of links to be activated without violation of interference constraints, and the transmission rate of each link. This work considers the FlashLinQ scheduler which was proposed by Qualcomm for scheduling in peer-to-peer ad-hoc networks [81]. The

scheduler is applied in a centralised case where a central network controller, possibly placed in the drone and with a view of the entire network makes routing and scheduling decisions. To mitigate the long end-to-end delay problem which characterize BP algorithms, Modified-BackPressure (M-BP) algorithms is proposed. M-BP takes into account the position of the control center (final destination receiver) when selecting the next hop for the drone-to-relay communication. Through extensive simulations the performance of the proposed algorithm is characterised in terms of delay and throughput, and compared with the selected benchmark BP algorithm.

The Back-Pressure (BP) algorithm, was proposed by Emphremides in [82] as routing and scheduling algorithm for multi-hop networks. In each time slot the algorithm performs both routing and scheduling decisions to forward packets from source to destination without relying on pre-computed routes [83]. Clearly, the algorithm is different from path-based routing protocols such as Dynamic Source Routing (DSR) [16] and Adhoc On Demand Distance Vector Routing (AODV) [17], which require routes between the source and destination nodes to be established before traffic forwarding can begin. In order to make the decisions, the algorithm relies on both queue backlog differential metric of links and channel state metric. Before traffic can start to flow from source to destination nodes there is need for pressure gradient which is created by having sufficient traffic in the network. Furthermore, the algorithm tries to exploit all possible paths in the network to enhance capacity of the network and mitigate congestion,. In fact BP was proved to be able to stabilize any traffic arrival rate vector within the network capacity region without the knowledge of channel state probabilities and arrival rates [82].

Due to its high throughput and the ability to adapt to the network dynamics,

the algorithm is expected to be applied widely in future radio networks such as in: high throughput and mobile IoTs [84], balancing resource usage in software-defined wireless backhauls of dense networks [85], routing and scheduling in software defined Wireless Sensor Networks [86], etc. However, there are some engineering challenges which limit its practical implementation in many scenarios of radio networks [83]. First, the algorithm can experience long end-to-end delays and especially in instances of low traffic load in the network because the pressure gradient needs to build up first in order for the algorithm to function properly. Second, the algorithm can result in large queues which may be unsupported in resource constrained devices such as in wireless Sensor Networks. The performance of the algorithm in different practical application scenario needs to be well studied and the existing issues resolved before its adoption.

5.2   Related Works

The backpressure algorithm was first introduced in [82] and has been widely studied in the context of multi-hop radio networks [87], software defined networks [85], IoT Networks [84], and cooperative relay network [88] and delay tolerant networks [89]. This algorithm can stabilize a queuing network with feasible arrival rate vector within the network capacity region. The algorithm was initially designed for centralised networks but it has been studied for decentralised radio networks such multi-hop CSMA-based networks [90].

Through Lyapunov drift and Lyapunov optimization techniques it has been shown in [91] that to stabilize the queue network (equivalent to minimizing the Lyapunov drift bound derived with quadratic functions of the queue backlogs) the weighted

maximization optimization problem given by equation (5.5.2) has to be solved at each time slot.

An extended Lyapunov drift theorem (i.e., drift plus penalty) is provided in [87]. The drift plus penalty methodology allows for design of backpressure algorithms which are able to trade-off queue backlog length with other network performance metrics such as delay, energy, packet loss rate etc. With this methodology a new function known as penalty function need to be appropriately designed and incorporated into the backpressure in order to achieve the desired trade-off in performance. For example the works provided by authors in [83] incorporates the expected number of transmissions (ETX) metric [20] as a penalty function to the backpressure scheme. In [92] authors propose a variant of algorithm which combines shortest path with backbressure in order to resolve the problem of high hop-count and long delays which occur under conditions of light load in the network. Backpressure Low power and Lossy Networks (BRPL) protocol for real-world industrial IoT applications is proposed in [84]. BRPL helps to resolve some of the well known performance issues of the RPL protocol such as: inability to cope with growing demands for high throughput, adaptability to data traffic dynamics, and mobility of IoT devices.

This work is is different from the above works because it is focused on the study of backpressure routing and scheduling scheme for drone monitoring application. The problem of link scheduling is addressed with FlashLinQ scheme which first proposed in [81] but never applied in the context of backpressure. Furthermore, new algorithm are proposed, which result to significant reduction in delay without loss of capacity as compared to the benchmark back-pressure algorithm.

5.3 Contribution and Structure of the Chapter

The contributions of this chapter can be summarised as follows:

- Backpressure and FlashLinQ algorithms are studied for a multi-hop scenario with a mobile drone and static relays.

- Modified BP algorithm, denoted as M-BP is proposed, which reduce end-to-end delay compared to the benchmark BP, while maintaining good throughput performance

The rest of the chapter is organised as follows: Section 5.4 decsribes the system model, Section 5.5 describes the BP and link schedulers, Section 5.6 describes the implementation, Section 5.7 discusses the numerical results, and finally Section 5.8 concludes the chapter.

5.4 System Model

5.4.1 Reference Scenario and traffic generation

Fig. 5.1 shows the scenario considered in this work, where a mobile drone is used to gather data from the environment and to transmit it to a remote control center in multi-hop. There are $\mathcal{N}$ static relays deployed randomly and uniformly on a square grid of side L, a single mobile drone, and a single control center. The drone flying at a speed of x [m/s], and at an altitude of h [m] above the ground, connects with ground relays via radio link. The drone generates traffic according to the Poisson distribution with mean rate of λ packets/slot.
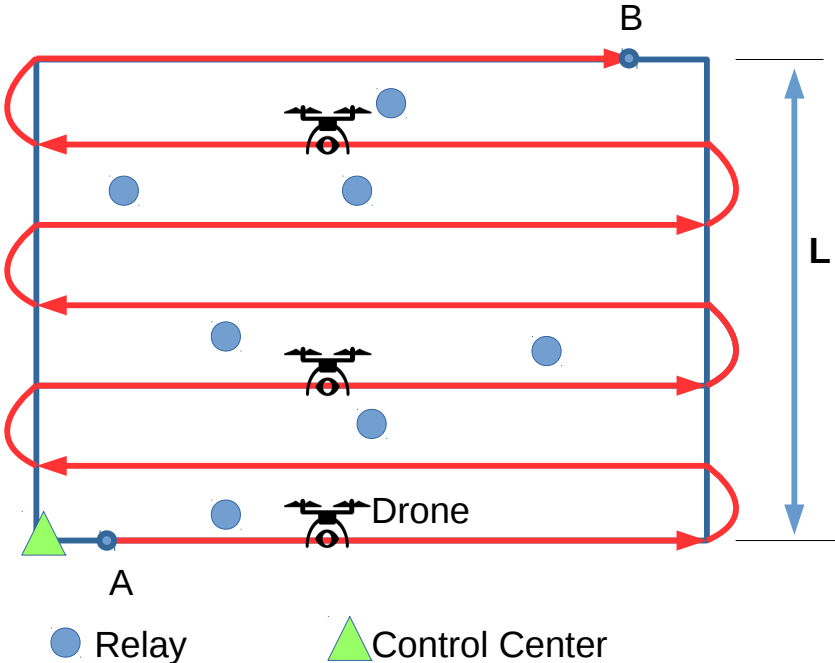
Figure 5.1: Reference Scenario.

Each node in the network has a set of queues denoted as $\mathcal{Q} = \{1, 2, ..n\}$ one for each of the **n** flows in the network. These queues evolve according to the equation (5.5.1). This chapter considers only a single flow network where the traffic source is the drone and the final destination is the control center.

5.4.2 Channel Model

In the scenario described above, there are two types of links: air-to-ground and ground-to-ground links. air-to-ground link represent drone-to-relay or drone-to-Control Center (CC) link, while ground-to-ground link is the relay-to-relay or relay-to-CC link. For the air-to-ground model the probabilistic channel model given in [93] is considered. According to this model, connections between drone and ground nodes can either be **Line of Sight (LOS)** or **Non Line of Sight (NLOS)**. When the connections occur in NLOS, the signals travel in LOS before interacting with objects located close to the ground which result in shadowing effect. Each node in the network under coverage experience LOS and NLOS connection with some probability denoted as $P(LOS)$ and $P(NLOS) = 1 - P(LOS)$ respectively. The LOS path loss model is given as

$$L_{LOS}(dB) = 20 \log(\frac{4\pi f_c d}{c}) + \zeta_{LOS} \tag{5.4.1}$$

On the other hand NLOS model is given as:

$$L_{NLOS}(dB) = 20 \log(\frac{4\pi f_c d}{c}) + \zeta_{NLOS} \tag{5.4.2}$$

where ζ is the shadowing coefficient which has Gaussian distribution, c is the speed of light, f_c is the center frequency, and d is the distance between the node and drone. The average path loss ($\overline{L}(R, h)$) is a function of the altitude of the drone (h)

and the ground coverage radius (R), and is given by

$$\overline{\mathbf{L}}(\mathbf{R}, \mathbf{h}) = \mathbf{P}(\mathbf{LOS}) \times \mathbf{L_{LOS}} + \mathbf{P}(\mathbf{NLOS}) \times \mathbf{L_{NLOS}} \qquad (5.4.3)$$

where $P(LOS)$ at a given elevation angle (θ) is computed according to the following equation

$$P(LOS) = \frac{1}{1 + \alpha \exp(-\beta[\frac{180}{\pi}\theta - \alpha])} \qquad (5.4.4)$$

with α and β being environment-dependent constants, i.e. rural. urban, dense urban, etc and adopted as given in [93]. The model for ground-to-ground path-loss, PL, is given by

$$PL = k_0 + k_1 log10(\frac{d}{d_0}) \qquad (5.4.5)$$

where k_0 is the reference path-loss computed at a reference distance $d_0 = 1$ m, from the transmitter. In the rest of the chapter k_0 is set to 40.7 dB. k_1 is the environment dependent path-loss exponent, and d is the distance of the receiver from the transmitter.

5.4.3   Mobility Models

The performance of routing protocols in ad-hoc networks depend on mobility patterns of nodes [94]. Therefore, performance characterisation of the protocols need to be done using appropriate models. The Paparazzi mobility (PPRZM) models [95], are the most appropriate for evaluating routing protocols in WMN with UAVs. These models are based on Paparazzi system for the UAVs developed and used at cole nationale de l'aviation civile (ENAC). This work considers the paparazzi model scan
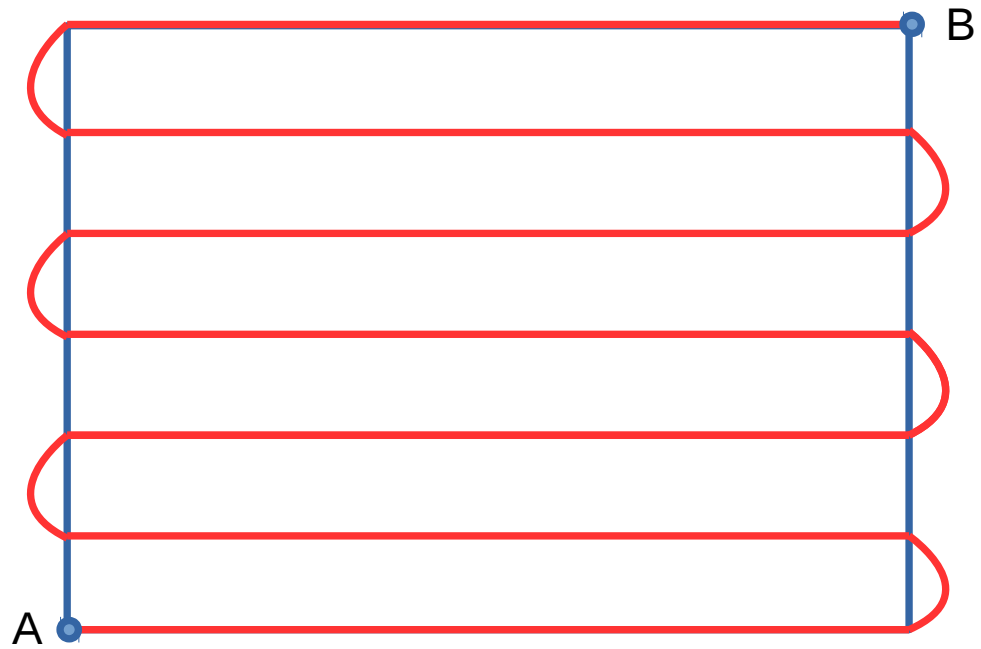
Figure 5.2: Paparazzi flight model with scan movement.

movement, where the drone scans a given area defined by two points along round trip trajectories as shown in Fig. 5.2

5.5 Algorithms

5.5.1 The BP Algorithm

The BP algorithm requires each node to maintain a set of queues one for each flow present in the network. During each time slot the algorithm performs two main tasks: flow scheduling and link scheduling. First, the algorithm decides which flow should be assigned to each of the links present in the network. Second, after flow scheduling, the algorithm has to decides a maximal subset of non-conflicting links to use the channel in a given slot. Each Queue in the network has the following dynamics:

$$Q(t+1) = max[Q(t) - \mu(t), 0] + A(t) \qquad (5.5.1)$$

where $Q(t)$ is the queue size at time instant t in units of bits or packets, $\mu(t)$ is the transmission rate of the outgoing link at time instant t, and $A(t)$ is the total number of arrivals in time t i.e., both endogenous and exogenous arrivals.

The BP algorithm is expressed as a weighted maximization problem given as:

$$\text{maximize} \quad \sum_{ab} W_{ab}(t) * f_{ab}(I(t), S(t))$$
$$\text{subject to} \quad I(t) \in \mathcal{I}_S(t) \qquad (5.5.2)$$

where W_{ab} is the optimal queue backlog differential of the selected flow on link ab during slot t, $f_{ab}(I(t), S(t) = \mu(t)$ is the rate of the link ab which depends on the network topology state $S(t)$ and the scheduling control action $I(t)$. The metric W_{ab}

is determined during the flow scheduling phase and it is computed in two steps as follows:

$$f_{ab}^* = \max_{f \in \mathcal{F}} \left[Q_a^f(t) - Q_b^f(t) \right] \tag{5.5.3}$$

$$W_{ab}^*(t) = \max \left[Q_a^{f_{ab}^*}(t) - Q_b^{f_{ab}^*}(t), 0 \right] \tag{5.5.4}$$

where f^* and $W_{ab}^*(t)$ are the optimal flow on the link ab and the optimal weight of the link at time t respectively. $\mathcal{F}$ is a set of all flows, and $Q_a^f(t)$ is the amount of packets of flow f on the node a at time t.

After determination of $W_{ab}^*(t)$ for each link in the network, the algorithm performs link scheduling. The optimal solution of the problem given by (5.5.2) is difficult to obtain since it is NP-hard, and therefore different greedy scheduling approaches are used to approximate the solution such as conflict graph scheduling.

As a **benchmark algorithm**, the BP algorithm is implemented.

5.5.2   Proposed Algorithms

The proposed algorithm is designed to reduce the long end-to-end delays suffered by the benchmark BP, while maintaining good throughput performance. Th algorithm is denoted as **M-BP**. With M-BP the drone selects the next-hop relays accounting for the position of the CC. The best next-hop relay for the drone is the one which is closest to the final destination provided that the drone is connected to it. Therefore, the drone maintains connectivity to its current receiver until it goes out of range. On the other hand, the static ground relays rely on backpressure to push the traffic to the final destination node. Therefore, M-BP is an hybrid algorithm which integrates two components: backpressure for relay-to-relay routing, and closest to the destination
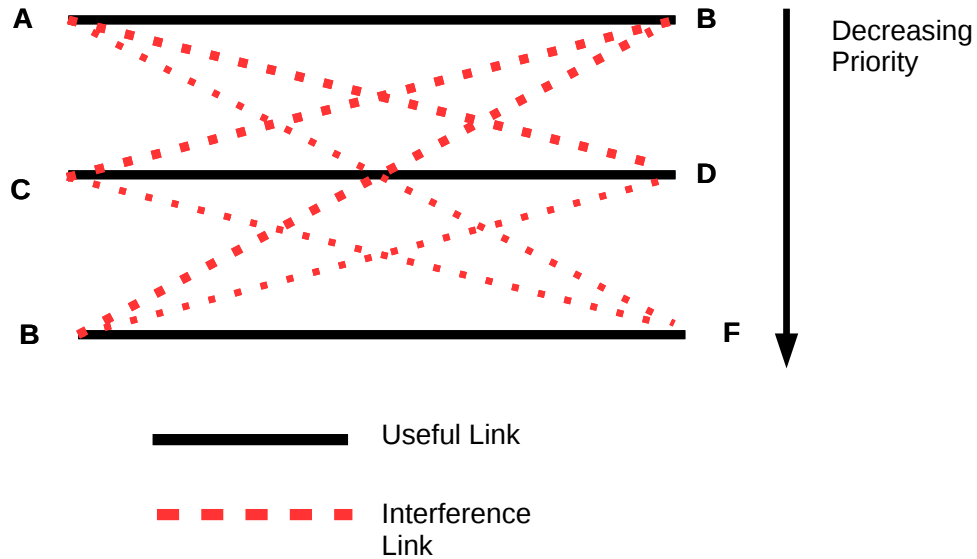
Figure 5.3: FlashLinQ scheduling with 3 links.

relay selection by the mobile drone. M-BP results in significant reduction in delay for different network settings in comparison with the benchmark backpressure without compromising throughput performance. The impact of reduced delay is due to two reasons: 1) the fact that, when the drone traffic is pushed close to the control center there are reduced chances of occurrence of long paths and/or loops in the network, 2) when a mobile drone transmits to a relay node closest to the CC, there are more chances of non-conflicting concurrent transmissions by the drone and relays close to the source because the drone keeps on moving away from those relays hence creating low interference.

5.5.3   FlashLinQ Scheduler

The FlashLinQ scheduling algorithm relies on the Signal to Interference Ratio (SIR) metric to derive a maximal subset of links which can be scheduled concurrently on the same channel in a given time slot without violating the protection ratio (minimum desired link SIR). The protection ratio is set according to the minimum desired data-rate in the network. In this work, the FlashLinQ algorithm applied in a centralized system, where the network controller mounted on the drones has a complete view of the entire network. The operation of the scheduler is as follows. First, the algorithm orders all links in decreasing order of priority as shown in Fig. 5.3. In this work, the priority metric is the queue backlog differential derived through the first phase of backpressure algorithm as described in Sec. 5.5.1, i.e., links are ordered in decreasing weight metric given by equation (5.5.4). Secondly, links are scheduled starting with higher priority links. A lower priority link is scheduled if its inclusion in the set of scheduled links does not violate the SIR constraint of any of the higher priority links and that of its own.

5.5.4   CSMA/CA with RTS/CTS

In order to benchmark the performance of FlashLinQ scheduler, the CSMA/CA with RTS/CTS is considered. CSMA/CA with RTS/CTS is a CSMA/CA protocol which is enhanced with short control packets, Request To Send (RTS) and Clear To Send (CTS), in order to mitigate the problem of hidden terminals in the network. With this type of CSMA/CA protocol it is easy to emulate scheduled transmissions by enforcing silence to all other transmitters within transmission range of the intended useful

105

Table 5.1: Default Parameters

Paramater	Value
β	0.28
α	9.6
λ	0.5 packet/slot
Drone Speed	10 m/s
Drone Height	20 m
Number of Relays	20
Relay transmit power	0 dBm
Drone transmit power	16 dBm
Noise Power	-104 dB
Protection Ratio	1.3 dB
Maximum queue limit	∞
Grid setting	5×5 nodes
CCA threshold	-95 dBm
k_1	3.0

transmitter and the receiver. Therefore, all transmitters within the transmission range of the intended transmitter and receiver remain silent in order to avoid collisions.

5.6   Simulator Setup and Performance Metrics

5.6.1   Simulator setup

For performance evaluation a custom C++ simulator was developed. The simulated scenario consists of a square field of length 1000 m, single drone flying at a speed of 10 m/s and height of 20 m above the ground. A variable number of relays are deployed on a fixed grid, and a single control center is fixed at the corner of the area. The diameter of the projected circular coverage area of the drone on the ground is 355 m (computation is based on the provided parameters and channel model). The trajectory of the drone is as reported in Fig. 5.2 and the channel model is implemented as reported in Sec. 5.4. The default parameters are summarized in Table 5.1.

Results are averaged over 100 scenarios with each scenario consisting of $10,000$ slots.

5.6.2   Performance metrics

1. Average Delay [slots]: Computed as the mean of the end-to-end delays of all received packets.

2. Throughput [packets/slot]: Computed as Total number of received packets by the control center divided by the total transmission time

Table 5.2: Backpressure with FlashLinQ and CSMA/CA schedulers

Algorithm	Throughput [packets/slot]
BP-FlashLinQ	0.4
BP-CSMA/CA	0.1

5.7 Numerical Results and Discussions

5.7.1 Comparison between FlashLinQ and CSMA/CA with RTS/CTS

The results reported in Tab. 5.2 compares the throughput performance of FlashLinQ and CSMA/CA with RTS/CTS schedulers. The results were obtained with benchmark BP algorithm and for a grid setting of 5×5 nodes. Moreover, for fair comparison between the two MAC protocols, all links were set to a fixed rate of 1 packet/slot i.e., no link rate adaptation was applied. In the table BP-FlashLinQ represents the performance of backpressure with FlashLInQ scheduler while BP-CSMA/CA represents the performance of backpressure with CSMA/CA scheduler. The results show that BP-FlashLinQ outperforms BP-CSMA/CA by 300% in terms of throughput achieved.

5.7.2 Comparison between BP and M-BP

This subsection reports the results for BP, M-BP algorithms. In this case all the algorithms implemented FlashLinQ as the link scheduler.

Figs. 5.4, 5.5, 5.6, and 5.7, Tabs. 5.3 and 5.4 compare the performance of **BP** and **M-BP**.
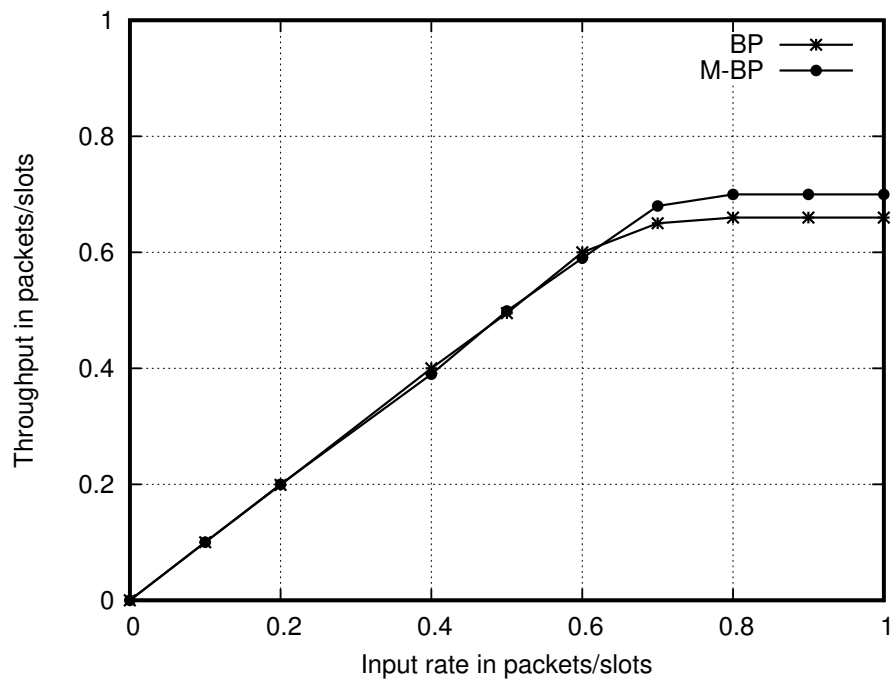
Figure 5.4: Throughput performance for different input rates
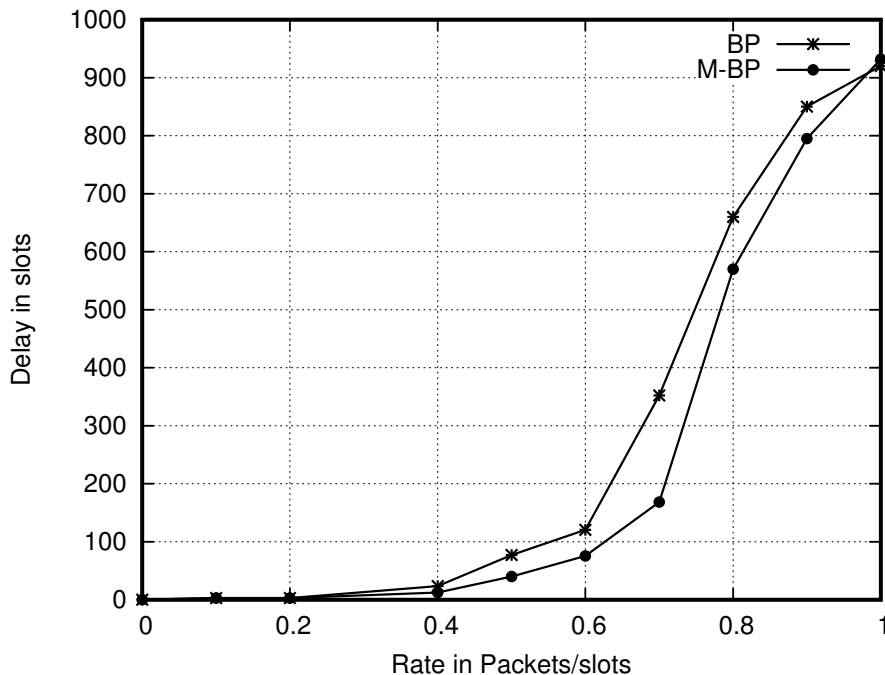
Figure 5.5: Delay performance for different input rates

Table 5.3: Average Number of Hops

Input rate	BP	M-BP
0.4	3.8	4.2
0.5	4.5	4.3

Fig. 5.4 shows how the throughput of the network changes when changing the input rate. As reported in the figure, network throughput increases linearly with input rate up to a maximum value and then saturates. Both the benchmark and the modified algorithms results in approximately the same throughput.

Fig. 5.5 compares the delay performance of the BP and M-BP. As a general trend, end-to-end delay increases with increasing input rate. This is because as the input rate increases, more packets have to wait in the queue for a longer time before they
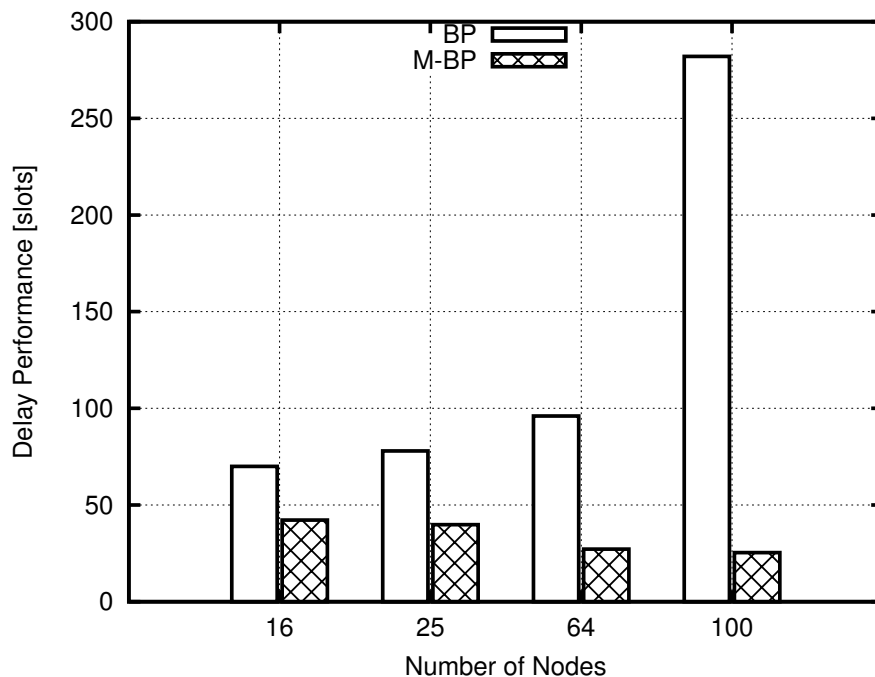
Figure 5.6: Variation of delay with increasing number of relays for $\lambda = 0.5$

can be scheduled and transmitted. Comparing the two algorithms, M-BP algorithm results into significant reduction in delay with respect to BP up to 52.2% when the input rate is fixed to 0.7 packets/slots. This reduction is due to the effect of the drone pushing its traffic to the relays close to the control center which in turn raises the chances of speedy delivery of packets to the control center. Similarly, the proposed algorithm results in lower average number of hops compared to the benchmark as reported in Tab. 5.3.

Fig. 5.6 compares the performance of the algorithms for different grid sizes, i.e., 4×4, 5×5, 8×8, and 10×10. As reported in the figure delay changes with the variation in the number of nodes deployed. The two algorithms exhibit inverse trends in that, delay increases for raising number of nodes for the benchmark backpressure
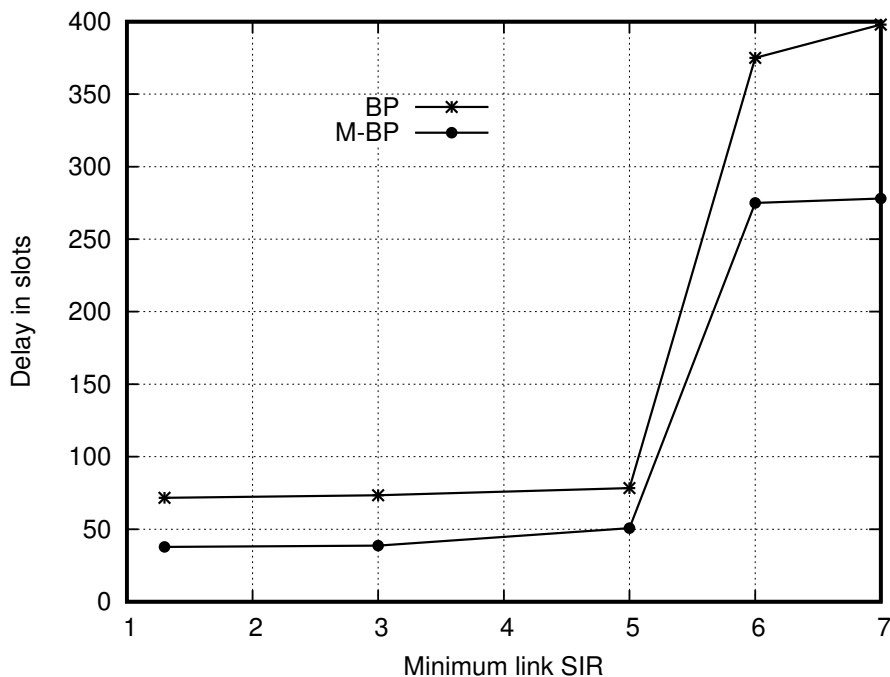
Figure 5.7: Effect of varying the minimum required SIR on delay when $\lambda = 0.5$

while for the modified backpressure delay decreases with raising number of nodes. This effect could be attributed to the fact that, for benchmark backpressure the traffic tries to spread in the entire network, while with modified backpressure as the number of relays increases the chances of the drone maintaining strong connectivity to nodes closer to the destination rises. This has an effect of ensuring faster delivery of packets since the pressure gradients of relays connected to the control center slopes towards the control center because its queue size is always zero.

Fig. 5.7 was obtained with 5×5 nodes grid setting and for a fixed input rate set to 0.5. The figure reports the effect of changing the minimum required link SIR metric on the delay performance. As a general trend, the end-to-end delay increases with raising minimum link SIR up to a maximum value. This is due to the fact

Table 5.4: Effect of maximum queue limit on performance when $\lambda = 0.7$ packets/slot

	BP		M-BP	
Queue size	**Delay**[slots]	**Throughput**[packets/slot]	**Delay**	**Throughput**
10	88.2	0.56	58.6	0.6
∞	402	0.66	164	0.70

that the number of non conflicting links supported within a single time slot increases with lowering of the minimum required transmission rate of the links. The delay performance for the M-BF is better than that of BP algorithm because M-BP allows the drone to push traffic close to the final destination and hence raises the chances of faster delivery of packets as compared to BP.

Tab. 5.4 reports the effect of limiting the maximum queue size on the throughput and delay performance. When the maximum queue limit is set to a lower value the delay performance of both algorithms is improved compared to when the maximum queue size is set to infinity. This is because of the effect of reduced queuing delay. However, this gain is attained at cost of increased packet dropping at the queues, and reduced throughput gain as reported in the same table.

5.8 Conclusion

In this chapter the performance of BP and M-BP have been reported. M-BP is a variant of the backpressure algorithm which is designed to mitigate the long end-to-end delays associated with backpressure. M-BP results in significant reduction of delay as compared to backpressure. Furthermore, the performance of FlashLinQ in the context of BP has been characterised and benchmarked with CSMA/CA with

RTS/CTS. It has been reported that flashLinQ results in 300% gain in throughput compared to CSMA/CA with RTS/CTS scheduler.

Chapter 6

Conclusions

In this thesis, two scenarios of future radio networks have been addressed: the coexistence of heterogeneous networks; and scenarios where drones are used for environmental monitoring. In respect to heterogeneous networks, Neigbors-Aware, Channel-Aware, and Coexistence-Aware algorithms were proposed for MAC, packet-length adaptation, and routing respectively. Through simulations it was demonstrated that, compared to the benchmark algorithms, the proposed algorithms significantly improve the performance of heterogeneous networks in terms of packet delivery rate and goodput without compromising the fairness index of the network. With reference to the topic on drones for environmental monitoring, routing protocols for WMN with drones were proposed and evaluated against the selected benchmark algorithms. First, a novel algorithm, denoted as O-HWMP, was proposed for video surveillance applications. Compared to the standard protocol RM-AODV for IEEE 802.11s standard, O-HWMP had better performance in terms of end-to-end delay, packet success rate and the video quality metric. Finally, backpressure routing and scheduling algorithms were applied the scenario and its performance characterised. In order to

improve on the long end-to-end delays resulting from the backpressure algorithm, a modified scheme denoted as, Modified backpressure, was proposed and evaluated.

Bibliography

[1] CISCO. Cisco visual networking index: Forecast and methodology, 20162021. June 2017.

[2] Q Wu, G Ding, Y Xu, S Feng, Z Du, J Wang, and K Long. Cognitive internet of things: A new paradigm beyond connection. *IEEE Internet of Things Journal*, 1(2):129–143, April 2014.

[3] Charles Jumaa Katila, Chiara Buratti, Melchiorre Danilo Abrignani, and Roberto Verdone. Neighbors-aware proportional fair scheduling for future wireless networks with mixed mac protocols. *EURASIP Journal on Wireless Communications and Networking*, 2017(1):93, May 2017.

[4] N Abramson. The aloha system: Another alternative for computer communications. In *Proceedings of the November 17-19, 1970, Fall Joint Computer Conference*, AFIPS '70 (Fall), pages 281–285, New York, NY, USA, 1970. ACM.

[5] LG Roberts. Aloha packet system with and without slots and capture. *SIGCOMM Comput. Commun. Rev.*, 5(2):28–42, April 1975.

[6] Y Wang and JJ Garcia-Luna-Aceves. Performance of collision avoidance protocols in single-channel ad hoc networks. In *Network Protocols, 2002. Proceedings. 10th IEEE International Conference on*, pages 68–77, Nov 2002.

[7] CL Fullmer and J. J. Garcia-Luna-Aceves. Solutions to hidden terminal problems in wireless networks. *SIGCOMM Comput. Commun. Rev.*, 27(4):39–49, October 1997.

[8] W. M. Moh, Dongming Yao, and K. Makki. Wireless lan: study of hidden-terminal effect and multimedia support. In *Proceedings 7th International Conference on Computer Communications and Networks (Cat. No.98EX226)*, pages 422–431, Oct 1998.

[9] Q Pang, A Bigloo, VCM Leung, and C Scholefield. Service scheduling for general packet radio service classes. In *WCNC*, 1999.

[10] C Wengerter, J Ohlhorst, and AGE von Elbwart. Fairness and throughput analysis for generalized proportional fair frequency scheduling in ofdma. In *2005 IEEE 61st Vehicular Technology Conference*, volume 3, pages 1903–1907 Vol. 3, May 2005.

[11] H. A. M. Ramli. Performance of maximum-largest weighted delay first algorithm in long term evolution-advanced with carrier aggregation. In *2014 IEEE Wireless Communications and Networking Conference (WCNC)*, pages 1415–1420, April 2014.

[12] I. Rhee, A. Warrier, M. Aia, J. Min, and M. L. Sichitiu. Z-mac: A hybrid mac for wireless sensor networks. *IEEE/ACM Transactions on Networking*, 16(3):511–524, June 2008.

[13] A. Ephremides and O. A. Mowafi. Analysis of a hybrid access scheme for buffered users-probabilistic time division. *IEEE Transactions on Software Engineering*, SE-8(1):52–61, Jan 1982.

[14] S. El Khediri, N. Nasri, A. Benfradj, A. Kachouri, and A. Wei. Routing protocols in manet: Performance comparison of aodv, dsr and dsdv protocols using ns2. In *The 2014 International Symposium on Networks, Computers and Communications*, pages 1–4, June 2014.

[15] Optimized link state routing protocol (OLSR), 2003.

[16] David B. Johnson, David A. Maltz, and Josh Broch. Ad hoc networking. chapter DSR: The Dynamic Source Routing Protocol for Multihop Wireless Ad Hoc Networks, pages 139–172. Addison-Wesley Longman Publishing Co., Inc., Boston, MA, USA, 2001.

[17] C. Perkins, E. Belding-Royer, and S. Das. Ad hoc on-demand distance vector (aodv) routing, 2003.

[18] Y. Yang and J. Wang. Design guidelines for routing metrics in multihop wireless networks. In *IEEE INFOCOM 2008 - The 27th Conference on Computer Communications*, April 2008.

[19] N. Javaid, M. Ullah, and K. Djouani. Identifying design requirements for wireless routing link metrics. In *2011 IEEE Global Telecommunications Conference - GLOBECOM 2011*, pages 1–5, Dec 2011.

[20] N. Javaid, A. Javaid, I. A. Khan, and K. Djouani. Performance study of etx based wireless routing metrics. In *2009 2nd International Conference on Computer, Control and Communication*, pages 1–7, Feb 2009.

[21] Richard Draves, Jitendra Padhye, and Brian Zill. Routing in multi-radio, multi-hop wireless mesh networks. In *Proceedings of the 10th Annual International Conference on Mobile Computing and Networking*, MobiCom '04, pages 114–128, New York, NY, USA, 2004. ACM.

[22] S. Filin, T. Baykas, H. Harada, F. Kojima, and H. Yano. Ieee standard 802.19.1 for tv white space coexis tence. *IEEE Communications Magazine*, 54(3):22–26, March 2016.

[23] Carlos Cordeiro, Kiran Challapali, Dagnachew Birru, and Sai Shankar N. IEEE 802.22: An Introduction to the First Wireless Standard based on Cognitive Radios. *Journal of Communications*, 1:38–47, 2006.

[24] M. H. Ng, S. D. Lin, J. Li, and S. Tatesh. Coexistence studies for 3gpp lte with other mobile systems. *IEEE Communications Magazine*, 47(4):60–65, April 2009.

[25] K. Ahmad, U. Meier, H. Kwasnicka, A. Pape, and B. Griese. A cognitive radio approach to realize coexistence optimized wireless automation systems. In *2009 IEEE Conference on Emerging Technologies Factory Automation*, pages 1–8, Sept 2009.

[26] W Song, MN Krishnan, and A Zakhor. Adaptive packetization for error-prone transmission over 802.11 wlans with hidden terminals. In *Multimedia Signal Processing, 2009. MMSP '09. IEEE International Workshop on*, pages 1–6, Oct 2009.

[27] Y Lin and VWS Wong. Wsn01-1: Frame aggregation and optimal frame size adaptation for ieee 802.11n wlans. In *IEEE Globecom 2006*, pages 1–6, Nov 2006.

[28] F Zheng and J Nelson. Adaptive design for the packet length of ieee 802.11n networks. In *2008 IEEE International Conference on Communications*, pages 2490–2495, May 2008.

[29] F. Mohammed, A. Idries, N. Mohamed, J. Al-Jaroodi, and I. Jawhar. Uavs for smart cities: Opportunities and challenges. In *2014 International Conference on Unmanned Aircraft Systems (ICUAS)*, pages 267–273, May 2014.

[30] A. Al-Hourani, S. Kandeepan, and A. Jamalipour. Modeling air-to-ground path loss for low altitude platforms in urban environments. In *2014 IEEE Global Communications Conference*, pages 2898–2904, Dec 2014.

[31] Alzenad. 3-d placement of an unmanned aerial vehicle base station (uav-bs) for energy-efficient maximal coverage. *IEEE Wireless Communications Letters*, 6(4):434–437, Aug 2017.

[32] Qualcomm. Leading the world to 5G: Evolving cellular technologies for safer drone operation.

[33] C. D. Franco and G. Buttazzo. Energy-aware coverage path planning of uavs. In *2015 IEEE International Conference on Autonomous Robot Systems and Competitions*, pages 111–117, April 2015.

[34] N. Bo, X. Li, J. Dai, and J. Tang. A hierarchical optimization strategy of trajectory planning for multi-uavs. In *2017 9th International Conference on Intelligent Human-Machine Systems and Cybernetics (IHMSC)*, volume 1, pages 294–298, Aug 2017.

[35] C. Cano and D. J. Leith. Unlicensed lte/wifi coexistence: Is lbt inherently fairer than csat? In *2016 IEEE International Conference on Communications (ICC)*, pages 1–6, May 2016.

[36] J. Mitola and G. Q. Maguire. Cognitive radio: making software radios more personal. *IEEE Personal Communications*, 6(4):13–18, Aug 1999.

[37] IEEE. IEEE Draft Standard for Information technology–Telecommunications and information exchange between systems Local and metropolitan area networks–Specific requirements Part 11: Wireless LAN Medium Access Control (MAC) and Physical Layer (PHY) Specifications. *IEEE P802.11-REVmc/D5.0, January 2016 (Revision of IEEE Std 802.11-2012 as amended by IEEE Std 802.11ae-2012, IEEE Std 802.11aa-2012, IEEE Std 802.11ad-2012, IEEE Std 802.11ac-2013, and IEEE Std 802.11af-2013)*, pages 1–3766, Jan 2016.

[38] C. Cano, D. Lopez-Perez, H. Claussen, and D. J. Leith. Using lte in unlicensed bands: Potential benefits and coexistence issues. *IEEE Communications Magazine*, 54(12):116–123, December 2016.

[39] C. Ghosh, S. Roy, and D. Cavalcanti. Coexistence challenges for heterogeneous cognitive wireless networks in tv white spaces. *IEEE Wireless Communications*, 18(4):22–31, August 2011.

[40] H. Li and Z. Han. Competitive spectrum access in cognitive radio networks: Graphical game and learning. In *2010 IEEE Wireless Communication and Networking Conference*, pages 1–6, April 2010.

[41] K. Bian, J. M. Park, L. Chen, and X. Li. Addressing the hidden terminal problem for heterogeneous coexistence between tdm and csma networks in white space. *IEEE Transactions on Vehicular Technology*, 63(9):4450–4463, Nov 2014.

[42] S. Bayhan and F. Alagoz. Scheduling in centralized cognitive radio networks for energy efficiency. *IEEE Transactions on Vehicular Technology*, 62(2):582–595, Feb 2013.

[43] L. Liu, X. Jin, G. Min, and K. Li. A comprehensive analytical model of cognitive radio networks employing centralized scheduling mechanism. In *2012 IEEE 14th*

International Conference on High Performance Computing and Communication 2012 IEEE 9th International Conference on Embedded Software and Systems, pages 1179–1184, June 2012.

[44] Xinyu Zhang and Kang G. Shin. Enabling coexistence of heterogeneous wireless systems: Case for zigbee and wifi. In *Proceedings of the Twelfth ACM International Symposium on Mobile Ad Hoc Networking and Computing,* MobiHoc '11, pages 6:1–6:11, New York, NY, USA, 2011. ACM.

[45] Cristina Cano, Douglas J. Leith, Andres Garcia-Saavedra, and Pablo Serrano. Fair coexistence of scheduled and random access wireless networks: Unlicensed lte/wifi. *CoRR,* abs/1605.00409, 2016.

[46] M. R. Palattella, N. Accettura, M. Dohler, L. A. Grieco, and G. Boggia. Traffic aware scheduling algorithm for reliable low-power multi-hop ieee 802.15.4e networks. In *2012 IEEE 23rd International Symposium on Personal, Indoor and Mobile Radio Communications - (PIMRC),* pages 327–332, Sept 2012.

[47] A Ephremides and OA Mowafi. Analysis of a hybrid access scheme for buffered users-probabilistic time division. *IEEE Transactions on Software Engineering,* SE-8(1):52–61, Jan 1982.

[48] B. Wang and K. J. R. Liu. Advances in cognitive radio networks: A survey. *IEEE Journal of Selected Topics in Signal Processing,* 5(1):5–23, Feb 2011.

[49] GA Shah and OB Akan. Spectrum-aware cluster-based routing for cognitive radio sensor networks. In *2013 IEEE International Conference on Communications (ICC),* pages 2885–2889, June 2013.

[50] Raj K. Jain. *The Art of Computer Systems Performance Analysis: Techniques for Experimental Design, Measurement, Simulation, and Modeling.* Wiley, 1 edition, April 1991.

[51] MC Vuran and IF Akyildiz. Cross-layer packet size optimization for wireless terrestrial, underwater, and underground sensor networks. In *INFOCOM 2008. The 27th Conference on Computer Communications. IEEE*, April 2008.

[52] MN Krishnan, S Pollin, and A Zakhor. Local estimation of probabilities of direct and staggered collisions in 802.11 wlans. In *GLOBECOM*, 2009.

[53] DG Yoon, SY Shin, JH Park, HS Park, and WH Kwon. *Performance Analysis of IEEE 802.11b Under Multiple IEEE 802.15.4 Interferences*, pages 213–222. Springer Berlin Heidelberg, Berlin, Heidelberg, 2007.

[54] A. Jamal, C. K. Tham, and W. C. Wong. Dynamic packet size optimization and channel selection for cognitive radio sensor networks. *IEEE Transactions on Cognitive Communications and Networking*, 1(4):394–405, Dec 2015.

[55] JH Kim and JK Lee. Capture effects of wireless csma/ca protocols in rayleigh and shadow fading channels. *IEEE Transactions on Vehicular Technology*, 48(4):1277–1286, Jul 1999.

[56] J Yang, Z Yifan, W Ying, and Z Ping. Average rate updating mechanism in proportional fair scheduler for hdr. In *Global Telecommunications Conference, 2004. GLOBECOM '04. IEEE*, volume 6, pages 3464–3466 Vol.6, Nov 2004.

[57] JI Choi, M Jain, MA Kazandjieva, and P Levis. Granting Silence to Avoid Wireless Collisions. In *Proceedings of the 18th IEEE International Conference on Network Protocols (ICNP)*, October 2010.

[58] R Jain, D Chiu, and WR Hawe. *A quantitative measure of fairness and discrimination for resource allocation in shared computer system.* Eastern Research Laboratory, Digital Equipment Corporation, 1984.

[59] Lijun Qian, Ning Song, D. R. Vaman, Xiangfang Li, and Z. Gajic. Power control and proportional fair scheduling with minimum rate constraints in clustered multihop td/cdma wireless ad hoc networks. In *IEEE Wireless Communications and Networking Conference, 2006. WCNC 2006.*, volume 2, pages 763–769, April 2006.

[60] G. Parissidis, M. Karaliopoulos, T. Spyropoulos, and B. Plattner. Interference-aware routing in wireless multihop networks. *IEEE Transactions on Mobile Computing*, 10(5):716–733, May 2011.

[61] S. A. Doomari and G. Mirjalily. Interference aware shortest route selection in energy constrained cognitive radio ad-hoc networks. In *2016 2nd International Conference of Signal Processing and Intelligent Systems (ICSPIS)*, pages 1–5, Dec 2016.

[62] U. Ullah, A. K. Kiani, R. F. Ali, and R. Ahmad. Network adaptive interference aware routing metric for hybrid wireless mesh networks. In *2016 International Wireless Communications and Mobile Computing Conference (IWCMC)*, pages 405–410, Sept 2016.

[63] H. Yuan, W. Guo, Y. Jin, S. Wang, and M. Ni. Interference-aware multi-hop path selection for device-to-device communications in a cellular interference environment. *IET Communications*, 11(11):1741–1750, 2017.

[64] E. W. Dijkstra. A note on two problems in connexion with graphs. *Numerische Mathematik*, 1:269–271, 1959.

[65] C. Buratti and R. Verdone. Joint routing and scheduling for centralised wireless sensor networks. In *2016 IEEE 2nd International Forum on Research and Technologies for Society and Industry Leveraging a better tomorrow (RTSI)*, pages 1–6, Sept 2016.

[66] Frank P Kelly, Aman K Maulloo, and David KH Tan. Rate control for communication networks: shadow prices, proportional fairness and stability. *Journal of the Operational Research society*, 49(3):237–252, 1998.

[67] S. Morgenthaler, T. Braun, Z. Zhao, T. Staub, and M. Anwander. Uavnet: A mobile wireless mesh network using unmanned aerial vehicles. In *2012 IEEE Globecom Workshops*, pages 1603–1608, Dec 2012.

[68] Silvio Sampaio, Pedro Souto, and Francisco Vasques. DCRP: a scalable path selection and forwarding scheme for IEEE 802.11s wireless mesh networks. *EURASIP Journal on Wireless Communications and Networking*, 2015(1):211, 2015.

[69] J. Pojda, A. Wolff, M. Sbeiti, and C. Wietfeld. Performance analysis of mesh routing protocols for uav swarming applications. In *2011 8th International Symposium on Wireless Communication Systems*, pages 317–321, Nov 2011.

[70] J. C. P. Wang, B. Hagelstein, and M. Abolhasan. Experimental evaluation of ieee 802.11s path selection protocols in a mesh testbed. In *2010 4th International Conference on Signal Processing and Communication Systems*, pages 1–3, Dec 2010.

[71] M. Mozaffari, W. Saad, M. Bennis, and M. Debbah. Drone small cells in the clouds: Design, deployment and performance analysis. In *2015 IEEE Global Communications Conference (GLOBECOM)*, pages 1–6, Dec 2015.

[72] L. Gupta, R. Jain, and G. Vaszkun. Survey of important issues in uav communication networks. *IEEE Communications Surveys Tutorials*, 18(2):1123–1152, Secondquarter 2016.

[73] P. M. Olsson, J. Kvarnstrm, P. Doherty, O. Burdakov, and K. Holmberg. Generating uav communication networks for monitoring and surveillance. In *2010 11th International Conference on Control Automation Robotics Vision*, pages 1070–1077, Dec 2010.

[74] O. K. Sahingoz. Mobile networking with uavs: Opportunities and challenges. In *2013 International Conference on Unmanned Aircraft Systems (ICUAS)*, pages 933–941, May 2013.

[75] K. Yang, J. f. Ma, and Z. h. Miao. Hybrid routing protocol for wireless mesh network. In *2009 International Conference on Computational Intelligence and Security*, volume 1, pages 547–551, Dec 2009.

[76] S. M. S. Bari, F. Anwar, and M. H. Masud. Performance study of hybrid wireless mesh protocol (hwmp) for ieee 802.11s wlan mesh networks. In *2012 International Conference on Computer and Communication Engineering (ICCCE)*, pages 712–716, July 2012.

[77] M. Cornils, M. Bahr, and T. Gamer. Simulative analysis of the hybrid wireless mesh protocol (hwmp). In *2010 European Wireless Conference (EW)*, pages 536–543, April 2010.

[78] M. X. Hu and G. S. Kuo. Delay and throughput analysis of ieee 802.11s networks. In *ICC Workshops - 2008 IEEE International Conference on Communications Workshops*, pages 73–78, May 2008.

[79] M. Stoffers and G. Riley. Comparing the ns-3 propagation models. In *2012 IEEE 20th International Symposium on Modeling, Analysis and Simulation of Computer and Telecommunication Systems*, pages 61–67, Aug 2012.

[80] Jirka Klaue, Berthold Rathke, and Adam Wolisz. *EvalVid – A Framework for Video Transmission and Quality Evaluation*, pages 255–272. Springer Berlin Heidelberg, Berlin, Heidelberg, 2003.

[81] X. Wu, S. Tavildar, S. Shakkottai, T. Richardson, J. Li, R. Laroia, and A. Jovicic. Flashlinq: A synchronous distributed scheduler for peer-to-peer ad hoc networks. *IEEE/ACM Transactions on Networking*, 21(4):1215–1228, Aug 2013.

[82] L. Tassiulas and A. Ephremides. Stability properties of constrained queueing systems and scheduling policies for maximum throughput in multihop radio networks. In *29th IEEE Conference on Decision and Control*, pages 2130–2132 vol.4, Dec 1990.

[83] Scott Moeller, Avinash Sridharan, Bhaskar Krishnamachari, and Omprakash Gnawali. Routing without routes: The backpressure collection protocol. In *Proceedings of the 9th ACM/IEEE International Conference on Information Processing in Sensor Networks*, IPSN '10, pages 279–290, New York, NY, USA, 2010. ACM.

[84] Y. Tahir, S. Yang, and J. McCann. Brpl: Backpressure rpl for high-throughput and mobile iots. *IEEE Transactions on Mobile Computing*, PP(99):1–1, 2017.

[85] J. Baranda, J. Nez-Martnez, and J. Mangues-Bafalluy. Applying backpressure to balance resource usage in software-defined wireless backhauls. In *2015 IEEE International Conference on Communication Workshop (ICCW)*, pages 31–36, June 2015.

[86] H. I. Kobo, A. M. Abu-Mahfouz, and G. P. Hancke. A survey on software-defined wireless sensor networks: Challenges and design requirements. *IEEE Access*, 5:1872–1899, 2017.

[87] Leonidas Georgiadis, Michael J. Neely, and Leandros Tassiulas. Resource allocation and cross-layer control in wireless networks. *Found. Trends Netw.*, 1(1):1–144, April 2006.

[88] E. Yeh and R. Berry. Throughput optimal control of wireless networks with two-hop cooperative relaying. In *2007 IEEE International Symposium on Information Theory*, pages 351–355, June 2007.

[89] M. Alresaini, M. Sathiamoorthy, B. Krishnamachari, and M. J. Neely. Backpressure with adaptive redundancy (bwar). In *2012 Proceedings IEEE INFOCOM*, pages 2300–2308, March 2012.

[90] M. Kurth and J. P. Redlich. Delay properties of opportunistic back-pressure routing in csma-based wireless mesh networks. In *2010 IEEE 21st International Symposium on Personal, Indoor and Mobile Radio Communications Workshops*, pages 479–484, Sept 2010.

[91] Michael J. Neely. *Stochastic Network Optimization with Application to Communication and Queueing Systems*. Morgan and Claypool Publishers, 2010.

[92] L. Ying, S. Shakkottai, and A. Reddy. On combining shortest-path and back-pressure routing over multihop wireless networks. In *IEEE INFOCOM 2009*, pages 1674–1682, April 2009.

[93] A. Al-Hourani, S. Kandeepan, and A. Jamalipour. Modeling air-to-ground path loss for low altitude platforms in urban environments. In *2014 IEEE Global Communications Conference*, pages 2898–2904, Dec 2014.

[94] Somsong Thounhom and Tanapat Anusas-amornkul. The study of routing protocols for uavs using paparazzi mobility model with different altitudes. In *Proceedings of the 2016 International Conference on Communication and Information Systems*, ICCIS '16, pages 106–111, New York, NY, USA, 2016. ACM.

[95] O. Bouachir, A. Abrassart, F. Garcia, and N. Larrieu. A mobility model for uav ad hoc network. In *2014 International Conference on Unmanned Aircraft Systems (ICUAS)*, pages 383–388, May 2014.

Publications

Reported research resulted in publications at international conferences and journals. They are summarised below.

- Journals

  - Charles Jumaa Katila, Chiara Buratti, Melchiorre Danilo Abrignani, and Roberto Verdone. **Neighbors-Aware Proportional Fair scheduling for future wireless networks with mixed MAC protocols**. EURASIP Journal on Wireless Communications and Networking 2017, no. 1 (2017): 93.

- Conferences:

  - Charles Jumaa Katila, Melchiorre Danilo Abrignani, and Roberto Verdone. **Neighbours-aware proportional fair scheduler for future wireless networks**. International Conference on Cognitive Radio Oriented Wireless Networks. Springer, Cham, 2016;

  - Charles Jumaa Katila, Antonio Di Gianni, Chiara Buratti, and Roberto Verdone. **Routing protocols for video surveillance drones in IEEE**

802.11 s Wireless Mesh Networks. In Networks and Communications (EuCNC), 2017 European Conference on, pp. 1-5. IEEE, 2017;

– Charles Jumaa Katila,and Chiara Buratti. **A Novel Routing and Scheduling Algorithm for Multi-hop Heterogeneous Wireless Networks**. **Submited to** : IEEE 87th Vehicular Technology Conference, 3-6 June 2018, Porto, Portugal;

– Katila, et al. **Back-pressure Routing and Scheduling for Multi-Hop Radio Networks with Droness**. **Submited to** ...

Acknowledgements